9-22-2010

Topological Defects and Gapless Modes in Insulators and Superconductors

Jeffrey C.Y. Teo
University of Pennsylvania, cteo@sas.upenn.edu

Charles L. Kane
University of Pennsylvania, kane@physics.upenn.edu

Suggested Citation:
Teo, J.C.Y. and C.L. Kane. (2010). "Topological defects and gapless modes in insulators and superconductors." *Physical Review B.* 82, 115120.

http://dx.doi.org/10.1103/PhysRevB.82.115120

Topological Defects and Gapless Modes in Insulators and Superconductors

Abstract
We develop a unified framework to classify topological defects in insulators and superconductors described by spatially modulated Bloch and Bogoliubov de Gennes Hamiltonians.We consider Hamiltonians $H(\mathrm{k},\mathrm{r})$ that vary slowly with adiabatic parameters r surrounding the defect and belong to any of the ten symmetry classes defined by time-reversal symmetry and particle-hole symmetry. The topological classes for such defects are identified and explicit formulas for the topological invariants are presented. We introduce a generalization of the bulk-boundary correspondence that relates the topological classes to defect Hamiltonians to the presence of protected gapless modes at the defect. Many examples of line and point defects in three-dimensional systems will be discussed. These can host one dimensional chiral Dirac fermions, helical Dirac fermions, chiral Majorana fermions, and helical Majorana fermions, as well as zero-dimensional chiral and Majorana zero modes. This approach can also be used to classify temporal pumping cycles, such as the Thouless charge pump, as well as a fermion parity pump, which is related to the Ising non-Abelian statistics of defects that support Majorana zero modes.

Disciplines
Physical Sciences and Mathematics | Physics

Comments
Suggested Citation:
Teo, J.C.Y. and C.L. Kane. (2010). "Topological defects and gapless modes in insulators and superconductors." *Physical Review B.* 82, 115120.

http://dx.doi.org/10.1103/PhysRevB.82.115120

PHYSICAL REVIEW B **82**, 115120 (2010)

Topological defects and gapless modes in insulators and superconductors

Jeffrey C. Y. Teo and C. L. Kane
Department of Physics and Astronomy, University of Pennsylvania, Philadelphia, Pennsylvania 19104, USA
(Received 3 June 2010; published 22 September 2010)

We develop a unified framework to classify topological defects in insulators and superconductors described by spatially modulated Bloch and Bogoliubov de Gennes Hamiltonians. We consider Hamiltonians $\mathcal{H}(\mathbf{k},\mathbf{r})$ that vary slowly with adiabatic parameters $\mathbf{r}$ surrounding the defect and belong to any of the ten symmetry classes defined by time-reversal symmetry and particle-hole symmetry. The topological classes for such defects are identified and explicit formulas for the topological invariants are presented. We introduce a generalization of the bulk-boundary correspondence that relates the topological classes to defect Hamiltonians to the presence of protected gapless modes at the defect. Many examples of line and point defects in three-dimensional systems will be discussed. These can host one dimensional chiral Dirac fermions, helical Dirac fermions, chiral Majorana fermions, and helical Majorana fermions, as well as zero-dimensional chiral and Majorana zero modes. This approach can also be used to classify temporal pumping cycles, such as the Thouless charge pump, as well as a fermion parity pump, which is related to the Ising non-Abelian statistics of defects that support Majorana zero modes.

DOI: 10.1103/PhysRevB.82.115120 PACS number(s): 73.20.−r, 73.43.−f, 71.10.Pm, 74.45.+c

I. INTRODUCTION

The classification of electronic phases according to topological invariants is a powerful tool for understanding and predicting the behavior of matter. This approach was pioneered by Thouless, *et al.*[1] (TKNN), who identified the integer topological invariant characterizing the two-dimensional (2D) integer quantum-Hall state. The TKNN invariant n gives the Hall conductivity $\sigma_{xy}=ne^2/h$ and characterizes the Bloch Hamiltonian $\mathcal{H}(\mathbf{k})$, defined as a function of $\mathbf{k}$ in the magnetic Brillouin zone. It may be expressed as the first Chern number associated with the Bloch wave functions of the occupied states. A fundamental consequence of this topological classification is the *bulk-boundary correspondence*, which relates the topological class of the bulk system to the number of gapless chiral fermion edge states on the sample boundary.

Recent interest in topological states[2–4] has been stimulated by the realization that the combination of time-reversal symmetry and the spin-orbit interaction can lead to topological insulating electronic phases[5–10] and by the prediction[11–13] and observation[14–26] of these phases in real materials. A topological insulator is a two- or three-dimensional material with a bulk energy gap that has gapless modes on the edge or surface that are protected by time-reversal symmetry. The bulk boundary correspondence relates these modes to a $\mathbb{Z}_2$ topological invariant characterizing time-reversal invariant Bloch Hamiltonians. Signatures of these protected boundary modes have been observed in transport experiments on 2D HgCdTe quantum wells[14–16] and in photoemission and scanning tunnel microscope experiments on three-dimensional (3D) crystals of $Bi_{1-x}Sb_x$,[17–19] Bi_2Se_3,[20] Bi_2Te_3,[22,23,25] and Sb_2Te_3.[26] Topological insulator behavior has also been predicted in other classes of materials with strong spin-orbit interactions.[27–33]

Superconductors, described within a Bogoliubov de Gennes (BdG) framework can similarly be classified topologically.[34–37] The Bloch-BdG Hamiltonian $\mathcal{H}_{\mathrm{BdG}}(\mathbf{k})$ has a structure similar to an ordinary Bloch Hamiltonian, except that it has an exact particle-hole symmetry that reflects the particle-hole redundancy inherent to the BdG theory. Topological superconductors are also characterized by gapless boundary modes. However, due to the particle-hole redundancy, the boundary excitations are Majorana fermions. The simplest model topological superconductor is a weakly paired spinless p wave superconductor in one-dimensional (1D),[38] which has zero-energy Majorana bound states at its ends. In 2D, a weakly paired p_x+ip_y superconductor has a chiral Majorana edge state.[39] Sr_2RuO_4 is believed to exhibit a triplet p_x+ip_y state.[40] The spin degeneracy, however, leads to a doubling of the Majorana edge states. Though undoubled topological superconductors remain to be discovered experimentally, superfluid ^{3}He B is a related topological phase[34,35,37,41,42] and is predicted to exhibit 2D gapless Majorana modes on its surface. Related ideas have also been used to topologically classify Fermi surfaces.[43]

Topological insulators and superconductors fit together into an elegant mathematical framework that generalizes the above classifications.[35,36] The topological classification of a general Bloch or BdG theory is specified by the dimension d and the ten Altland-Zirnbauer symmetry classes[44] characterizing the presence or absence of particle-hole, time-reversal, and/or chiral symmetry. The topological classifications, given by $\mathbb{Z}$, $\mathbb{Z}_2$, or 0 show a regular pattern as a function of symmetry class and d, and can be arranged into a *periodic table* of topological insulators and superconductors. Each nontrivial entry in the table is predicted, via the bulk-boundary correspondence, to have gapless boundary states.

Topologically protected zero modes and gapless states can also occur at topological defects, and have deep implications in both field theory and condensed matter physics.[41,45–47] A simple example is the zero-energy Majorana mode that occurs at a vortex in a p_x+ip_y superconductor.[39] Similar Majorana bound states can be engineered using three dimensional heterostructures that combine ordinary superconductors and topological insulators,[48] as well as semiconductor structures

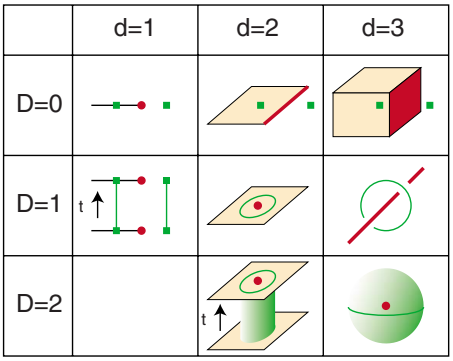

FIG. 1. (Color online) Topological defects characterized by a D parameter family of d-dimensional Bloch-BdG Hamiltonians. Line defects correspond to $d-D=2$ while point defects correspond to $d-D=1$. Temporal cycles for point defects correspond to $d-D=0$.

that combine superconductivity, magnetism, and strong spin-orbit interactions.[49–52] Recently, we showed that the existence of a Majorana bound state at a point defect in a three dimensional Bogoliubov de Gennes theory is related to a $\mathbb{Z}_2$ topological invariant that characterizes a family of Bogoliubov de Gennes Hamiltonians $\mathcal{H}_{\mathrm{BdG}}(\mathbf{k},\mathbf{r})$ defined for $\mathbf{r}$ on a surface surrounding the defect.[53] This suggests that a more general formulation of topological defects and their corresponding gapless modes should be possible.

In this paper we develop a general theory of topological defects and their associated gapless modes in Bloch and Bloch-BdG theories in all symmetry classes. As in Ref. 53, we assume that far away from the defect the Hamiltonian varies slowly in real space, allowing us to consider adiabatic changes in the Hamiltonian as a function of the real space position $\mathbf{r}$. We thus seek to classify Hamiltonians $\mathcal{H}(\mathbf{k},\mathbf{r})$, where $\mathbf{k}$ is defined in a d-dimensional Brillouin zone (a torus T^d), and $\mathbf{r}$ is defined on a D-dimensional surface S^D surrounding the defect. A similar approach can be used to classify cyclic temporal variations in the Hamiltonian, which define adiabatic pumping cycles. Hereafter we will drop the BdG subscript on the Hamiltonian with the understanding that the symmetry class dictates whether it is a Bloch or BdG Hamiltonian.

In Fig. 1 we illustrate the types of topological defects that can occur in $d=1$, 2, or 3. For $D=0$ we regard S^0 as two points ($\{-1,+1\}$). Our topological classification then classifies the *difference* of $\mathcal{H}(\mathbf{k},+1)$ and $\mathcal{H}(\mathbf{k},-1)$. A nontrivial difference corresponds to an interface between two topologically distinct phases. For $D=1$ the one parameter families of Hamiltonians describe line defects in $d=3$ and point defects in $d=2$. For $d=1$ it could correspond to an adiabatic temporal cycle $H(\mathbf{k},t)$. Similarly for $D=2$, the two parameter family describes a point defect for $d=3$ or an adiabatic cycle for a point defects in $d=2$.

Classifying the D parameter families of d-dimensional Bloch-BdG Hamiltonians subject to symmetries leads to a generalization of the periodic table discussed above. The original table corresponds to $D=0$. For $D>0$ we find that for a given symmetry class the topological classification ($\mathbb{Z}$, $\mathbb{Z}_2$, or 0) depends only on

$$\delta = d - D. \tag{1.1}$$

Thus, all line defects with $\delta=2$ have the same topological classification, irrespective of d, as do point defects with $\delta=1$ and pumping cycles with $\delta=0$. Though the classifications depend only on δ, the *formulas* for the topological invariants depend on both d and D.

This topological classification of $\mathcal{H}(\mathbf{k},\mathbf{r})$ suggests a generalization of the bulk-boundary correspondence that relates the topological class of the Hamiltonian characterizing the defect to the structure of the protected modes associated with the defect. This has a structure reminiscent of a mathematical *index theorem*[54] that relates a topological index to an analytical index that counts the number of zero modes.[41,45,46,55–59] In this paper we will not attempt to *prove* the index theorem. Rather, we will observe that the topological classes for $\mathcal{H}(\mathbf{k},\mathbf{r})$ coincide with the expected classes of gapless defect modes. In this regards the dependence of the classification on δ in Eq. (1.1) is to be expected. For example, a point defect at the end of a one-dimensional system ($\delta=1-0$) has the same classification as a point defects in two dimensions ($\delta=2-1$) and three dimensions ($\delta=3-2$).

We will begin in Sec. II by describing the generalized periodic table. We will start with a review of the Altland Zirnbauer symmetry classes[44] and a summary of the properties of the table. In Appendix A we will justify this generalization of the table by introducing a set of mathematical mappings that relate Hamiltonians in different dimensions and different symmetry classes. In addition to establishing that the classifications depend only on $\delta=d-D$, these mappings allow other features of the table, already present for $D=0$ to be easily understood, such as the pattern in which the classifications vary as a function of symmetry class as well as the Bott periodicity of the classes as a function of d.

In Secs. III and IV we will outline the physical consequences of this theory by discussing a number of examples of line and point defects in different symmetry classes and dimensions. The simplest example is that of a line defect in a 3D system with no symmetries. In Sec. III A we will show that the presence of a 1D *chiral Dirac fermion* mode (analogous to an integer quantum-Hall edge state) on the defect is associated with an integer topological invariant that may be interpreted as the winding number of the "θ" term that characterizes the magnetoelectric polarizability.[10] This description unifies a number of methods for "engineering" chiral Dirac fermions, which will be described in several illustrative examples.

Related topological invariants and illustrative examples will be presented in Secs. III B–III E for line defects in other symmetry classes that are associated with gapless 1D helical Dirac fermions, 1D chiral Majorana fermions, and 1D helical Majorana fermions. In Sec. IV we will consider point defects in 1D models with chiral symmetry such as the Jackiw-Rebbi model[45] or the Su, Schrieffer, Heeger model,[47] and in superconductors without chiral symmetry that exhibit Majorana bound states or Majorana doublets. These will also be related to the early work of Jackiw and Rossi[46] on Majorana modes at point defects in a model with chiral symmetry.

TABLE I. Periodic table for the classification of topological defects in insulators and superconductors. The rows correspond to the different Altland Zirnbauer (AZ) symmetry classes while the columns distinguish different dimensionalities, which depend only on $\delta=d-D$.

Symmetry					$\delta=d-D$							
s	AZ	Θ^2	Ξ^2	Π^2	0	1	2	3	4	5	6	7
0	A	0	0	0	$\mathbb{Z}$	0	$\mathbb{Z}$	0	$\mathbb{Z}$	0	$\mathbb{Z}$	0
1	AIII	0	0	1	0	$\mathbb{Z}$	0	$\mathbb{Z}$	0	$\mathbb{Z}$	0	$\mathbb{Z}$
0	AI	1	0	0	$\mathbb{Z}$	0	0	0	$2\mathbb{Z}$	0	$\mathbb{Z}_2$	$\mathbb{Z}_2$
1	BDI	1	1	1	$\mathbb{Z}_2$	$\mathbb{Z}$	0	0	0	$2\mathbb{Z}$	0	$\mathbb{Z}_2$
2	D	0	1	0	$\mathbb{Z}_2$	$\mathbb{Z}_2$	$\mathbb{Z}$	0	0	0	$2\mathbb{Z}$	0
3	DIII	−1	1	1	0	$\mathbb{Z}_2$	$\mathbb{Z}_2$	$\mathbb{Z}$	0	0	0	$2\mathbb{Z}$
4	AII	−1	0	0	$2\mathbb{Z}$	0	$\mathbb{Z}_2$	$\mathbb{Z}_2$	$\mathbb{Z}$	0	0	0
5	CII	−1	−1	1	0	$2\mathbb{Z}$	0	$\mathbb{Z}_2$	$\mathbb{Z}_2$	$\mathbb{Z}$	0	0
6	C	0	−1	0	0	0	$2\mathbb{Z}$	0	$\mathbb{Z}_2$	$\mathbb{Z}_2$	$\mathbb{Z}$	0
7	CI	1	−1	1	0	0	0	$2\mathbb{Z}$	0	$\mathbb{Z}_2$	$\mathbb{Z}_2$	$\mathbb{Z}$

Finally, in Sec. V we will regard $\mathbf{r}$ as including a temporal variable, and apply the considerations in this paper to classify cyclic pumping processes. The Thouless charge pump[60,61] corresponds to a nontrivial cycle in a system with no symmetries and $\delta=0$ ($d=D=1$). A similar pumping scenario can be applied to superconductors and defines a *fermion parity pump*. This, in turn, is related to the non-Abelian statistics of Ising anyons and provides a framework for understanding braidless operations on systems of three-dimensional superconductors hosting Majorana fermion bound states. Details of several technical calculations can be found in the Appendices. An interesting recent preprint by Freedman *et al.*,[62] which appeared when this manuscript was in its final stages discusses some aspects of the classification of topological defects in connection with a rigorous theory of non-Abelian statistics in higher dimensions.

II. PERIODIC TABLE FOR DEFECT CLASSIFICATION

Table I shows the generalized periodic table for the classification of topological defects in insulators and superconductors. It describes the equivalence classes of Hamiltonians $\mathcal{H}(\mathbf{k},\mathbf{r})$, that can be continuously deformed into one another without closing the energy gap, subject to constraints of particle-hole and/or time-reversal symmetry. These are mappings from a *base space* defined by $(\mathbf{k},\mathbf{r})$ to a *classifying space*, which characterizes the set of gapped Hamiltonians. In order to explain the table, we need to describe (i) the symmetry classes, (ii) the base space, (iii) the classifying space, and (iv) the notion of stable equivalence. The repeating patterns in the table will be discussed in Sec. II C. Much of this section is a review of material in Refs. 35 and 36. What is new is the extension to $D>0$.

A. Symmetry classes

The presence or absence of time reversal symmetry, particle-hole symmetry, and/or chiral symmetry define the ten Altland-Zirnbauer symmetry classes.[44] Time-reversal symmetry implies that

$$\mathcal{H}(\mathbf{k},\mathbf{r}) = \Theta\mathcal{H}(-\mathbf{k},\mathbf{r})\Theta^{-1}, \tag{2.1}$$

where the antiunitary time reversal operator may be written $\Theta=e^{i\pi S^y/\hbar}K$. S^y is the spin and K is complex conjugation. For spin-1/2 fermions, $\Theta^2=-1$, which leads to Kramers theorem. In the absence of a spin-orbit interaction, the extra invariance of the Hamiltonian under rotations in spin space allows an additional time-reversal operator $\Theta'=K$ to be defined, which satisfies $\Theta'^2=+1$.

Particle-hole symmetry is expressed by

$$\mathcal{H}(\mathbf{k},\mathbf{r}) = -\Xi\mathcal{H}(-\mathbf{k},\mathbf{r})\Xi^{-1}, \tag{2.2}$$

where Ξ is the antiunitary particle-hole operator. Fundamentally, $\Xi^2=+1$. However, as was the case for Θ, the absence of spin-orbit interactions introduces an additional particle-hole symmetry, which can satisfy $\Xi^2=-1$.

Finally, chiral symmetry is expressed by a unitary operator Π, satisfying

$$\mathcal{H}(\mathbf{k},\mathbf{r}) = -\Pi\mathcal{H}(\mathbf{k},\mathbf{r})\Pi^{-1}. \tag{2.3}$$

A theory with both particle-hole and time-reversal symmetries automatically has a chiral symmetry $\Pi=e^{i\chi}\Theta\Xi$. The phase χ can be chosen so that $\Pi^2=1$.

Specifying $\Theta^2=0,\pm1$, $\Xi^2=0,\pm1$, and $\Pi^2=0,1$ (here 0 denotes the absence of symmetry) defines the ten Altland-Zirnbauer symmetry classes. They can be divided into two groups: eight *real* classes that have anti unitary symmetries Θ and or Ξ plus two *complex* classes that do not have anti unitary symmetries. Altland and Zirnbauer's notation for these classes, which is based on Cartan's classification of symmetric spaces, is shown in the left-hand part of Table I.

To appreciate the mathematical structure of the eight real symmetry classes it is helpful to picture them on an 8 h "clock," as shown in Fig. 2. The x and y axes of the clock represent the values of Ξ^2 and Θ^2. The "time" on the clock can be represented by an integer s defined modulo 8. Kitaev[36] used a slightly different notation to label the symmetry classes. In his formulation, class D is described by a real Clifford algebra with no constraints, and in the other

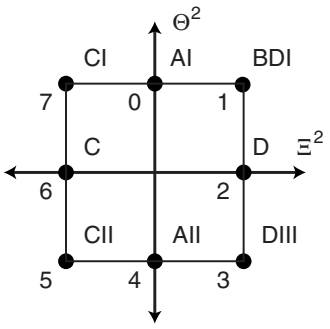

FIG. 2. The eight real symmetry classes that involve the antiunitary symmetries Θ (time reversal) and/or Ξ (particle hole) are specified by the values of $\Theta^2=\pm 1$ and $\Xi^2=\pm 1$. They can be visualized on an eight-hour "clock."

classes Clifford algebra elements are constrained to anticommute with q positive generators. The two formulations are related by $s=q+2$ mod 8. The complex symmetry classes can similarly be indexed by an integer s defined modulo 2. For all classes, the presence of chiral symmetry is associated with odd s.

B. Base space, classifying space and stable equivalence

The Hamiltonian is defined on a base space composed of momentum $\mathbf{k}$, defined in a d-dimensional Brillouin zone T^d and real-space degrees of freedom $\mathbf{r}$ in a sphere S^D (or $S^{D-1}\times S^1$ for an adiabatic cycle). The total base space is therefore $T^d\times S^D$ (or $T^d\times S^{D-1}\times S^1$). As in Ref. 36, we will simplify the topological classification by treating the base space as a sphere S^{d+D}. The "strong" topological invariants that characterize the sphere will also characterize $T^d\times S^D$. However, there may be additional topological structure in $T^d\times S^D$ that is absent in S^{d+D}. These correspond to "weak" topological invariants. For $D=0$ these arise in layered structures. A weak topological insulator, for example, can be understood as a layered two dimensional topological insulator. There are similar layered quantum-Hall states. For $D\neq 0$, then there will also be a weak invariant if the Hamiltonian $\mathcal{H}(\mathbf{k},\mathbf{r}_0)$ for fixed $\mathbf{r}=\mathbf{r}_0$ is topologically nontrivial. As is the case for the classification of bulk phases $D=0$, we expect that the topologically protected gapless defect modes are associated with the strong topological invariants.

The set of Hamiltonians that preserve the energy gap separating positive and negative energy states can be simplified without losing any topological information. Consider the retraction of the original Hamiltonian $\mathcal{H}(\mathbf{k},\mathbf{r})$ to a simpler Hamiltonian whose eigenvalue spectrum is "flattened" so that the positive- and negative-energy states all have the same energy $\pm E_0$. The flattened Hamiltonian is then specified the set of all n eigenvectors [defining a $U(n)$ matrix] modulo unitary rotations within the k conduction bands or the $n-k$ valence bands. The flattened Hamiltonian can thus be identified with a point in the Grassmanian manifold

$$G_{n,k}=U(n)/U(k)\times U(n-k). \tag{2.4}$$

It is useful to broaden the notion of topological equivalence to allow for the presence of extra trivial energy bands. Two families of Hamiltonians are *stably equivalent* if they can be deformed into one another after adding an arbitrary number of trivial bands. Thus, trivial insulators with different numbers of core energy levels are stably equivalent. Stable equivalence can be implemented by considering an expanded *classifying space* that includes an infinite number of extra conduction and valence bands, $\mathcal{C}_0=U/U\times U\equiv\cup_{k=0}^{\infty}G_{\infty,k}$.

With this notion of stable equivalence, the equivalence classes of Hamiltonians $\mathcal{H}(\mathbf{k},\mathbf{r})$ can be formally added and subtracted. The addition of two classes, denoted $[\mathcal{H}_1]+[\mathcal{H}_2]$ is formed by simply combining two independent Hamiltonians into a single Hamiltonian given by the matrix direct sum, $[\mathcal{H}_1\oplus\mathcal{H}_2]$. Additive inverses are constructed through reversing conduction and valence bands, $[\mathcal{H}_1]-[\mathcal{H}_2]=[\mathcal{H}_1\oplus-\mathcal{H}_2]$. $[\mathcal{H}\oplus-\mathcal{H}]$ is guaranteed to the be trivial class [0]. Because of this property, the stable equivalence classes form an Abelian group, which is the key element of K theory.[63–65]

Symmetries impose constraints on the classifying space. For the symmetry classes with chiral symmetry, Eq. (2.3) restricts $n=2k$ and the classifying space to a subset $\mathcal{C}_1=U(\infty)\subset U/U\times U$. The antiunitary symmetries in Eqs. (2.1) and (2.2) impose further constraints. At the special points where $\mathbf{k}$ and $-\mathbf{k}$ coincide, the allowed Hamiltonians are described by the 8 classifying spaces $\mathcal{R}_q$ of real K theory.

C. Properties of the periodic table

For a given symmetry class s, the topological classification of defects is given by the set of stable equivalence classes of maps from the base space $(\mathbf{k},\mathbf{r})\in S^{D+d}$ to the classifying space, subject to the symmetry constraints. These form the K group, which we denote as $K_{\mathbb{C}}(s;D,d)$ for the complex symmetry classes and $K_{\mathbb{R}}(s;D,d)$ for the real symmetry classes. These are listed in Table I.

Table I exhibits many remarkable patterns. Many can be understood from the following basic periodicities:

$$K_{\mathbb{F}}(s;D,d+1)=K_{\mathbb{F}}(s-1;D,d), \tag{2.5}$$

$$K_{\mathbb{F}}(s;D+1,d)=K_{\mathbb{F}}(s+1;D,d). \tag{2.6}$$

Here s is understood to be defined modulo 2 for $\mathbb{F}=\mathbb{C}$ and modulo 8 for $\mathbb{F}=\mathbb{R}$. We will establish these identities mathematically in Appendix A. The basic idea is to start with some Hamiltonian in some symmetry class s and dimensionalities D and d. It is then possible to explicitly construct two new Hamiltonians in one higher dimension which have either (i) $d\to d+1$ or (ii) $D\to D+1$. These new Hamiltonians belongs to new symmetry classes that are shifted by 1 "hour" on the symmetry clock and characterized by (i) $s\to s+1$ or (ii) $s\to s-1$. We then go on to show that this construction defines a 1–1 correspondence between the equivalence classes of Hamiltonians with the new and old symmetry classes and dimensions, thereby establishing Eqs. (2.5) and (2.6).

The periodicities in Eqs. (2.5) and (2.6) have a number of consequences. The most important for our present purposes is they can be combined to give

$$K_{\mathbb{F}}(s;D+1,d+1)=K_{\mathbb{F}}(s;D,d). \tag{2.7}$$

This (1,1) periodicity shows that the dependence on the dimensions d and D only occurs via $\delta=d-D$. Thus the dependence of the classifications on D can be deduced from the table for $D=0$. This is one of our central results.

In addition, the periodicities in Eqs. (2.5) and (2.6) explain other features of the table that are already present for $D=0$. In particular, the fact that s is defined modulo 2 (8) for the complex (real) classes leads directly to the Bott periodicity of the dependence of the classifications on d

$$K_{\mathbb{C}}(s;D,d+2)=K_{\mathbb{C}}(s;D,d), \tag{2.8}$$

$$K_{\mathbb{R}}(s;D,d+8)=K_{\mathbb{R}}(s;D,d). \tag{2.9}$$

Moreover, Eqs. (2.5) and (2.6) show that $K_a(s;D,d)$ depends only on $d-D-s$. This explains the diagonal pattern in Table I, in which the dependence of the classification on d is repeated in successive symmetry classes. Thus, the entire table could be deduced from a single row.

Equations (2.5) and (2.6) do not explain the pattern of classifications within a single row. Since this is a well-studied math problem there are many routes to the answer.[64,66,67] One approach is to notice that for $d=0$, $K_{\mathbb{F}}(s,D,0)$ is simply the Dth homotopy group of the appropriate classifying space which incorporates the symmetry constraints. For example, for class BDI ($s=1$, $\Xi^2=+1$, and $\Theta^2=+1$) the classifying space is the orthogonal group $O(\infty)$. Then, $K_{\mathbb{R}}(1,D,0)=\pi_D[O(\infty)]$, which are well known. This implies

$$K_{\mathbb{R}}(s;D,d)=\pi_{s+D-d-1}[O(\infty)]. \tag{2.10}$$

Additional insight can be obtained by examining the interconnections between different elements of the table. For example, the structure within a column can be analyzed by considering the effect of "forgetting" symmetries. Hamiltonians belonging to the real chiral (nonchiral) classes are automatically in complex class AIII (A). There are therefore K group homomorphisms that send any real entries in Table I to complex ones directly above. In particular, as detailed in Appendix B this distinguishes the $\mathbb{Z}$ and $2\mathbb{Z}$ entries, which indicate the possible values of Chern numbers [or $U(n)$ winding numbers] for even (or odd) δ. In addition, the dimensional reduction arguments given in Refs. 10 and 68 lead to a dimensional hierarchy, which helps to explain the pattern within a single row as a function of d.

III. LINE DEFECTS

Line defects can occur at the edge of a 2D system ($\delta=2-0$) or in a 3D system ($\delta=3-1$). From Table I, it can be seen that there are five symmetry classes which can host nontrivial line defects. These are expected to be associated with gapless fermion modes bound to the defect. Table II lists nontrivial classes, along with the character of the associated gapless modes. In the following sections we will discuss each of these cases, along with physical examples.

TABLE II. Symmetry classes that support topologically nontrivial line defects and their associated protected gapless modes.

Symmetry	Topological classes	1D gapless Fermion modes
A	$\mathbb{Z}$	Chiral Dirac
D	$\mathbb{Z}$	Chiral Majorana
DIII	$\mathbb{Z}_2$	Helical Majorana
AII	$\mathbb{Z}_2$	Helical Dirac
C	$2\mathbb{Z}$	Chiral Dirac

A. Class A: Chiral Dirac fermion

1. Topological invariant

A line defect in a generic 3D Bloch band theory with no symmetries is associated with an integer topological invariant. This determines the number of chiral Dirac fermion modes associated with the defect. Since $\mathcal{H}(\mathbf{k},\mathbf{r})$ is defined on a compact four-dimensional space, this invariant is naturally expressed as a second Chern number

$$n=\frac{1}{8\pi^2}\int_{T^3\times S^1}\mathrm{Tr}[\mathcal{F}\wedge\mathcal{F}], \tag{3.1}$$

where

$$\mathcal{F}=d\mathcal{A}+\mathcal{A}\wedge\mathcal{A} \tag{3.2}$$

is the curvature form associated with the non-Abelian Berry's connection $\mathcal{A}_{ij}=\langle u_i|du_j\rangle$ characterizing the valence-band eigenstates $|u_j(\mathbf{k},s)\rangle$ defined on the loop S^1 parameterized by s.

It is instructive to rewrite this as an integral over s of a quantity associated with the local band structure. To this end, it is useful to write $\mathrm{Tr}[\mathcal{F}\wedge\mathcal{F}]=d\mathcal{Q}_3$, where the Chern-Simons 3 form is

$$\mathcal{Q}_3=\mathrm{Tr}\left[\mathcal{A}\wedge d\mathcal{A}+\frac{2}{3}\mathcal{A}\wedge\mathcal{A}\wedge\mathcal{A}\right]. \tag{3.3}$$

Now divide the integration volume into thin slices, $T^3\times\Delta S^1$, where ΔS^1 is the interval between s and $s+\Delta s$. In each slice, Stokes' theorem may be used to write the integral as a surface integral over the surfaces of the slice at s and $s+\Delta s$. In this manner, Eq. (3.1) may be written

$$n=\frac{1}{2\pi}\oint_{S^1}ds\frac{d}{ds}\theta(s), \tag{3.4}$$

where

$$\theta(s)=\frac{1}{4\pi}\int_{T^3}\mathcal{Q}_3(\mathbf{k},s). \tag{3.5}$$

Equation (3.5) is precisely the Qi, Hughes, and Zhang formula[10] for the "θ" term that characterizes the magnetoelectric response of a band insulator. $\theta=0$ for an ordinary time reversal invariant insulator, and $\theta=\pi$ in a strong topological insulator. If parity and time-reversal symmetry are broken then θ can have any intermediate value. We thus conclude that the topological invariant associated with a line

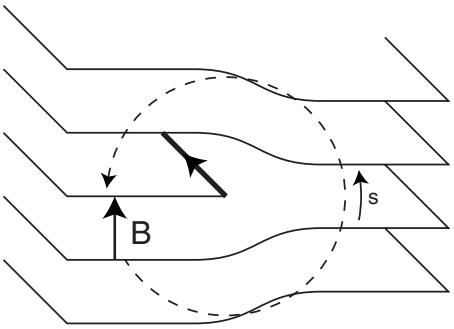

FIG. 3. A line dislocation in a three-dimensional quantum-Hall state characterized by Burgers vector **B**.

defect, which determines the number of chiral fermion branches is given by the winding number of θ. We now consider several examples of 3D line defects that are associated with chiral Dirac fermions.

2. Dislocation in a 3D integer quantum-Hall state

A three-dimensional integer quantum-Hall state can be thought of as a layered version of the two-dimensional integer quantum-Hall state. This can be understood most simply by considering the extreme limit where the layers are completely decoupled 2D systems. A line dislocation, as shown in Fig. 3 will then involve an edge of one of the planes and be associated with a chiral fermion edge state. Clearly, the chiral fermion mode will remain when the layers are coupled, provided the bulk gap remains finite. Here we wish to show how the topological invariant in Eq. (3.1) reflects this fact.

On a loop surrounding the dislocation parameterized by $s \in [0,1]$ we may consider a family of Hamiltonians $H(\mathbf{k},s)$ given by the Hamiltonian of the original bulk crystal displaced by a distance $s\mathbf{B}$, where $\mathbf{B}$ is a lattice vector equal to the Burgers vector of the defect. The corresponding Bloch wave functions will thus be given by

$$u_{m\mathbf{k},s}(\mathbf{r}) = u^0_{m\mathbf{k}}(\mathbf{r} - s\mathbf{B}), \tag{3.6}$$

where $u^0_{m\mathbf{k}}(\mathbf{r})$ are Bloch functions for the original crystal. It then follows that the Berry's connection is

$$\mathcal{A} = \mathcal{A}^0 + \mathbf{B} \cdot [\mathbf{k} - \mathbf{a}^p(\mathbf{k})]ds, \tag{3.7}$$

where

$$\mathcal{A}^0_{mn}(\mathbf{k}) = \langle u^0_{m\mathbf{k}} | \nabla_{\mathbf{k}} | u^0_{n\mathbf{k}} \rangle \cdot d\mathbf{k}$$

and

$$\mathbf{a}^p_{mn}(\mathbf{k}) = \langle u^0_{m\mathbf{k}} | (\nabla_{\mathbf{r}} + \mathbf{k}) | u^0_{n\mathbf{k}} \rangle. \tag{3.8}$$

With this definition, $\mathbf{a}^p(\mathbf{k})$ is a periodic function: $\mathbf{a}^p(\mathbf{k}+\mathbf{G}) = \mathbf{a}^p(\mathbf{k})$ for any reciprocal lattice vector $\mathbf{G}$.[69]

If the crystal is in a three dimensional quantum-Hall state, then the nonzero first Chern number is an obstruction to finding the globally continuous gauge necessary to evaluate Eq. (3.5). We therefore use Eq. (3.1), which can be evaluated by noting that

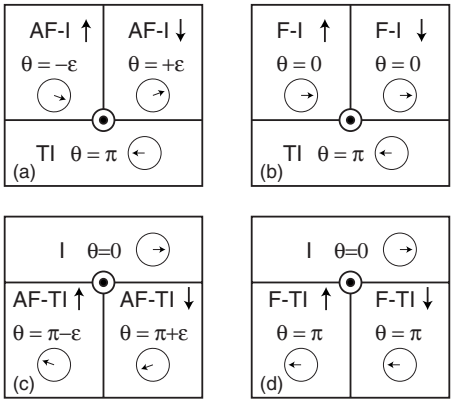

FIG. 4. Heterostructure geometries for chiral Dirac fermions. (a) and (b) show antiferromagnetic or ferromagnetic insulators on the surface of a topological insulator with chiral Dirac fermions at a domain wall. (c) and (d) show a domain wall in an antiferromagnetic or ferromagnetic topological insulator. Chiral fermion modes are present when the domain wall intersects the surface.

$$\mathrm{Tr}[\mathcal{F} \wedge \mathcal{F}] = \mathrm{Tr}[\mathbf{B} \cdot (2\mathcal{F}^0 \wedge d\mathbf{k} - d[\mathcal{F}^0, \mathbf{a}^p]) \wedge ds]. \tag{3.9}$$

Upon integrating $\mathrm{Tr}[\mathcal{F} \wedge \mathcal{F}]$ the total derivative term vanishes due to the periodicity of $\mathbf{a}^p$. Evaluating the integral is then straightforward. The integral over s trivially gives 1. We are then left with

$$n = \frac{1}{2\pi}\mathbf{B} \cdot \mathbf{G}_c, \tag{3.10}$$

where

$$\mathbf{G}_c = \frac{1}{2\pi}\int_{T^3} d\mathbf{k} \wedge \mathrm{Tr}[\mathcal{F}^0]. \tag{3.11}$$

$\mathbf{G}_c$ is a reciprocal lattice vector that corresponds to the triad of Chern numbers that characterize a 3D system. For instance, in a cubic system $\mathbf{G}_c = (2\pi/a)(n_x, n_y, n_z)$, where, for example $n_z = (2\pi)^{-1}\int \mathrm{Tr}[\mathcal{F}^0_{xy}]dk_x \wedge dk_y$, for any value of k_z.

An equivalent formulation is to characterize the displaced crystal in terms of θ. Though Eq. (3.5) cannot be used, Eqs. (3.1) and (3.4) can be used to implicitly define θ up to an arbitrary additive constant

$$\theta(s) = s\mathbf{B} \cdot \mathbf{G}_c. \tag{3.12}$$

3. Topological insulator heterostructures

Another method for engineering chiral Dirac fermions is use heterostructures that combine topological insulators and magnetic materials. The simplest version is a topological insulator coated with a magnetic film that opens a time-reversal symmetry breaking energy gap at the surface. A domain wall is then associated with a chiral fermion mode. In this section we will show how this structure, along with some variants on the theme, fits into our general framework. We first describe the structures qualitatively and then analyze a model that describes them.

Figure 4 shows four possible configurations. Figures 4(a) and 4(b) involve a topological insulator with magnetic mate-

rials on the surface. The magnetic material could be either ferromagnetic or antiferromagnetic. We distinguish these two cases based on whether inversion symmetry is broken or not. Ferromagnetism does not violate inversion symmetry while antiferromagnetism does (at least for inversion about the middle of a bond). This is relevant because θ, discussed above, is quantized unless *both* time reversal and inversion symmetries are violated. Of course, for a noncentrosymmetric crystal inversion is already broken so the distinction is unnecessary.

Figure 4(a) shows a topological insulator capped with antiferromagnetic insulators with $\theta = \pm\epsilon$ separated by a domain wall. Around the junction where the three regions meet θ cycles between π, $+\epsilon$, and $-\epsilon$. Of course this interface structure falls outside the adiabatic regime that Eq. (3.5) is based on. However, it is natural to expect that the physics would not change if the interface was "smoothed out" with θ taking the shortest smooth path connecting its values on either side of the interface.

Figure 4(b) shows a similar device with ferromagnetic insulators, for which $\theta=0$ or π. In this case the adiabatic assumption again breaks down, however, as emphasized in Ref. 10, the appropriate way to think about the surface is that θ connects 0 and π along a path that is determined by the sign of the induced gap, which in turn is related to the magnetization. In this sense, θ cycles by 2π around the junction.

In Figs. 4(c) and 4(d) we consider topological insulators which have a weak magnetic instability. If in addition to time-reversal, inversion symmetry is broken, then $\theta \sim \pi \pm \epsilon$. Recently Li, Wang, Qi, and Zhang[70] have considered such materials in connection with a theory of a dynamical axion and suggested that certain magnetically doped topological insulators may exhibit this behavior. They referred to such materials as topological magnetic insulators. We prefer to call them *magnetic topological insulators* because as magnetic insulators they are topologically trivial. Rather, they are topological insulators to which magnetism is added. Irrespective of the name, such materials would be extremely interesting to study, and as we discuss below, may have important technological utility.

Figure 4(c) shows two antiferromagnetic topological insulators with $\theta = \pi \pm \epsilon$ separated by a domain wall, and Fig. 4(d) shows a similar device with ferromagnetic topological insulators. They form an interface with an insulator, which could be vacuum. Under the same continuity assumptions as above the junction where the domain wall meets the surface will be associated with a chiral fermion mode. Like the structure in Fig. 4(a), this may be interpreted as an edge state on a domain wall between the "half-quantized" quantum-Hall states of the topological insulator surfaces. However, an equally valid interpretation is that the domain wall itself forms a single two-dimensional integer quantum-Hall state with an edge state. Our framework for topologically classifying the line defects underlies the equivalence between these two points of view.

Mong, Essen, and Moore[71] have introduced a *different* kind of antiferromagnetic topological insulator that relies on the symmetry of time reversal combined with a lattice translation. Due to the necessity of translation symmetry, however, such a phase is not robust to disorder. They found that chiral Dirac modes occur at certain step edges in such crystals. These chiral modes can also be understood in terms of the invariant in Eq. (3.1). Note that these chiral modes survive in the presence of disorder even though the bulk state does not. Thus, the chiral mode, protected by the strong invariant in Eq. (3.1), is more robust than the bulk state that gave rise to it.

If one imagines weakening the coupling between the two antiferromagnetic topological insulators (using our terminology, not that of Mong, *et al.*[71]) and taking them apart, then at some point the chiral mode has to disappear. At that point, rather than taking the "shortest path" between $\pi \pm \epsilon$, θ takes a path that passes through 0. At the transition between the "short-path" and the "long-path" regimes, the gap on the domain wall must go to zero, allowing the chiral mode to escape. This will have the character of a plateau transition in the 2D integer quantum-Hall effect.

Structures involving magnetic topological insulators would be extremely interesting to study because with them it is possible to create chiral fermion states with a single material. Indeed, one can imagine scenarios where a magnetic memory, encoded in magnetic domains, could be read by measuring the electrical transport in the domain wall chiral fermions.

To model the chiral fermions in these structures we begin with the simple three-dimensional model for trivial and topological insulators considered in Ref. 10

$$\mathcal{H}_0 = v\mu_x \vec{\sigma}\cdot\mathbf{k} + (m + \epsilon|\mathbf{k}|^2)\mu_z. \tag{3.13}$$

Here $\vec{\sigma}$ represents spin and μ_z describes an orbital degree of freedom. $m>0$ describes the trivial insulator and $m<0$ describes the topological insulator. An interface where m changes sign is then associated with gapless surface states.

Next consider time-reversal symmetry-breaking perturbations, which could arise from exchange fields due to the presence of magnetic order. Two possibilities include

$$\mathcal{H}_{af} = h_{af}\mu_y, \tag{3.14}$$

$$\mathcal{H}_f = \vec{h}_f\cdot\vec{\sigma}. \tag{3.15}$$

Either h_{af} or $h_{f,z}$ will introduce a gap in the surface states but they have different physical content. $\mathcal{H}_0$ has an inversion symmetry given by $\mathcal{H}_0(\mathbf{k}) = P\mathcal{H}_0(-\mathbf{k})P$ with $P=\mu_z$. Clearly, $\mathcal{H}_f$ respects this inversion symmetry. $\mathcal{H}_{af}$ does not respect P but does respect $P\Theta$. We therefore associate $\mathcal{H}_f$ with ferromagnetic order and $\mathcal{H}_{af}$ with antiferromagnetic order.

Within the adiabatic approximation, the topological invariant in Eq. (3.1) can be evaluated in the presence of either Eq. (3.14) or (3.15). The antiferromagnetic perturbation in Eq. (3.14) is most straightforward to analyze because $\mathcal{H}_0 + H_{af}$ is a combination of five anticommuting Dirac matrices. On a circle surrounding the junction parameterized by s it can be written in the general form

$$H(\mathbf{k},s) = \mathbf{h}(\mathbf{k},s)\cdot\vec{\gamma}, \tag{3.16}$$

where $\vec{\gamma} = (\mu_x\sigma_x, \mu_x\sigma_y, \mu_x\sigma_z, \mu_z, \mu_y)$ and $\mathbf{h}(\mathbf{k},s) = [v\mathbf{k}, m(s) + \epsilon|\mathbf{k}|^2, h_{af}(s)]$. For a model of this form, the second Chern number in Eq. (3.1) is given simply by the winding number

of the unit vector $\hat{\mathbf{d}}(\mathbf{k},s)=\mathbf{h}/|\mathbf{h}| \in S^4$ as a function of $\mathbf{k}$ and s. This is most straightforward to evaluate in the limit $\epsilon \to 0$, where $\hat{\mathbf{d}}$ is confined to the "equator" $(d_1,d_2,d_3,0,0)$ everywhere except near $\mathbf{k}\sim 0$ and $|\mathbf{k}| \gtrsim 1/\epsilon$. The winding number is determined by the behavior at $\mathbf{k}\sim 0$, and may be expressed by Eq. (3.4) with θ given by

$$e^{i\theta}=\frac{m+ih_{af}}{\sqrt{m^2+h_{af}^2}}. \tag{3.17}$$

We therefore expect a topological line defect to occur at an intersection between planes where m and h_{af} change sign. The chiral fermion mode associated with this defect can seen explicitly if we solve a simple linear model, $m=f_z z$, $h_{af}=f_y y$. This model, which has the form of a harmonic oscillator, is solved in Appendix C, and explicitly gives the chiral Dirac fermion mode with dispersion

$$E(k_x)=v\ \mathrm{sgn}(f_z f_y)k_x. \tag{3.18}$$

B. Class D: Chiral Majorana fermions

1. Topological invariant

A line defect in a superconductor without time-reversal symmetry is characterized by an integer topological invariant that determines the number of associated chiral Majorana fermion modes. Since the BdG Hamiltonian characterizing a superconductor has the same structure as the Bloch Hamiltonian, we can analyze the problem by "forgetting" about the particle-hole symmetry and treating the BdG Hamiltonian as if it was a Bloch Hamiltonian. The second Chern number, given by Eq. (3.1) can be defined. It can be verified that any value of the Chern number is even under particle-hole symmetry so that particle-hole symmetry does not rule out a nonzero Chern number. We may follow the same steps as Eqs. (3.1)–(3.5) to express the integer topological invariant as

$$\tilde{n}=\frac{1}{8\pi^2}\int_{T^3\times S^1}\mathrm{Tr}[\tilde{\mathcal{F}}\wedge\tilde{\mathcal{F}}], \tag{3.19}$$

where $\tilde{\mathcal{F}}$ is the curvature form characterizing the BdG theory. As in Eq. (3.4), $\tilde{n}$ may be expressed as a winding number of $\tilde{\theta}$, which is expressed as an integral over the Brillouin zone of the Chern-Simons 3 form. The difference between n and $\tilde{n}$ is that $\tilde{n}$ characterizes a BdG Hamiltonian. If we considered the BdG Hamiltonian for a nonsuperconducting insulator, then due to the doubling in the BdG equation, we would find

$$\tilde{n}=2n. \tag{3.20}$$

In this case, the chiral Dirac fermion that occurs for a 2π $(n=1)$ winding of θ corresponds to a 4π $(n=2)$ winding of $\tilde{\theta}$. Superconductivity allows for the possibility of a 2π winding in $\tilde{\theta}$: a chiral Dirac fermion can be split into a pair of chiral Majorana fermions.

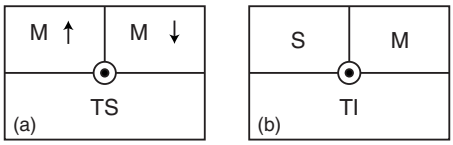

FIG. 5. Heterostructure geometries for Chiral Majorana fermions. (a) shows a magnetic domain wall on the surface of a topological superconductor while (b) shows an interface between a superconductor and a magnet on the surface of a topological insulator.

2. Dislocation in a layered topological superconductor

The simplest example to consider is a dislocation in a three-dimensional superconductor. The discussion closely parallels Sec. III A 2 and we find

$$\tilde{n}=\frac{1}{2\pi}\mathbf{B}\cdot\tilde{\mathbf{G}}_c, \tag{3.21}$$

where $\mathbf{B}$ is the Burgers vector of the dislocation and $\tilde{\mathbf{G}}_c$ characterizes the triad of first Chern numbers characterizing the 3D BdG Hamiltonian. A 3D system consisting of layers of a 2D topological superconductor will be characterized by a nonzero $\tilde{\mathbf{G}}_c$. Since, as a 3D superconductor, the layered structure is in the topologically trivial class, such a state could be referred to as a *weak topological superconductor*.

The simplest model system in this class is a stack of 2D p_x+ip_y superconductors. A dislocation would then have $\tilde{n}=1$ and a single chiral Majorana fermion branch. A possible physical realization of the weak topological superconductor state is Sr_2RuO_4, which may exhibit triplet p_x+ip_y pairing. Since the spin-up and spin-down electrons make two copies of the spinless state, a dislocation will be associated with $\tilde{n}=2$. Thus, we predict that there will be two chiral Majorana modes bound to the dislocation, which is the same as a single chiral Dirac fermion mode.

3. Superconductor heterostructures

We now consider heterostructures with associated chiral Majorana modes. The simplest to consider is a BdG analog of the structures considered in Fig. 5. These would involve, for example, an interface between a 3D time-reversal invariant topological superconductor with a magnetic material with a magnetic domain wall. The analysis of such a structure is similar to that in Eq. (3.13) if we replace the Pauli matrices describing the orbital degree of freedom $\vec{\mu}$ with Pauli matrices describing Nambu space $\vec{\tau}$. Protected chiral Majorana fermion modes of this sort on the surface of ^{3}He-B with a magnetic domain wall have been recently discussed by Volovik.[72]

In Ref. 48 a different method for engineering chiral Majorana fermions was introduced by combining an interface between superconducting and magnetic regions on the surface of a topological insulator. To describe this requires the eight-band model introduced in Ref. 53

$$H=\tau_z\mu_x\vec{\sigma}\cdot\mathbf{k}+(m+\epsilon|\mathbf{k}|^2)\tau_z\mu_z+\Delta\tau_x+h\mu_y. \tag{3.22}$$

(Here, for simplicity we consider only the antiferromagnetic term). The surface of the topological insulator occurs at a

domain wall (say, in the x-y plane), where $m(z)$ changes sign. The superconducting order parameter Δ and magnetic perturbation h both lead to an energy gap in the surface states. This Hamiltonian is straightforward to analyze because $[\mathcal{H}, \tau_x \mu_y]=0$, which allows the 8×8 problem to be divided into two 4×4 problems, which have superconducting/magnetic mass terms $\Delta \pm h$. Near a defect where $\Delta=h$ the $\Delta+h$ gap never closes while the $\Delta-h$ gap can be critical. $\Delta>h$ leads to a superconducting state while $\Delta<h$ leads to a quantum-Hall-type state. There is a transition between the two at $\Delta=h$.

An explicit model for the line defect can be formulated with $m(z)=f_z z$, $\Delta-h=f_y y$ and $\Delta+h=M$. The topological invariant in Eq. (3.19) can be evaluated using a method similar to Eq. (3.16) and the chiral Majorana states can be explicitly solved along the lines of Eq. (3.18).

C. Class AII: Helical Dirac fermions

1. Topological invariant

Line defects for class AII are characterized by a $\mathbb{Z}_2$ topological invariant. To develop a formula for this invariant we follow the approach used in Ref. 73 to describe the invariant characterizing the quantum spin-Hall insulator.

As in the previous section, a line defect in three dimensions is associated with a four parameter space $(\mathbf{k},\mathbf{r}) \in T^3 \times S^1$. Due to time-reversal symmetry, the second Chern number that characterized the line defects in Eq. (3.1) must be zero. Thus there is no obstruction to defining Bloch basis functions $|u(\mathbf{k},\mathbf{r})\rangle$ continuously over the entire base space. However, the time reversal relation between $(-\mathbf{k},\mathbf{r})$ and $(\mathbf{k},\mathbf{r})$ allows for an additional constraint so that the state is specified by the degrees of freedom in *half* the Brillouin zone.

As in Ref. 73 it is useful to define a matrix

$$w_{mn}(\mathbf{k},\mathbf{r}) = \langle u_m(\mathbf{k},\mathbf{r})|\Theta|u_n(-\mathbf{k},\mathbf{r})\rangle. \tag{3.23}$$

Because $|u_m(\mathbf{k},\mathbf{r})\rangle$ and $|u_n(-\mathbf{k},\mathbf{r})\rangle$ are related by time-reversal symmetry $w(\mathbf{k},\mathbf{r})$ is a unitary matrix that depends on the gauge choice for the basis functions. Locally it is possible to choose a basis in which

$$w(\mathbf{k},\mathbf{r}) = w_0, \tag{3.24}$$

where w_0 is independent of $\mathbf{k}$ and $\mathbf{r}$ so that states at $(\pm\mathbf{k},\mathbf{r})$ have a fixed relation. Since for $\mathbf{k}=0$ $w=-w^T$, w_0 must be antisymmetric. A natural choice is thus $w_0=i\sigma_2\otimes 1$.

The $\mathbb{Z}_2$ topological invariant is an obstruction to finding such a constrained basis globally. The constrained basis can be defined on two patches but the basis functions on the two patches are necessarily related by a topologically nontrivial transition function. In this sense, the $\mathbb{Z}_2$ invariant resembles the second Chern number in Eq. (3.1).

In Appendix E we will generalize the argument developed in Ref. 73 to show that the transition function relating the two patches defines the $\mathbb{Z}_2$ topological invariant, which may be written[74]

$$\nu = \frac{1}{8\pi^2}\left(\int_{(1/2)T^3\times S^1} \mathrm{Tr}[\mathcal{F}\wedge\mathcal{F}] - \int_{\partial(1/2)T^3\times S^1} \mathcal{Q}_3\right) \mathrm{mod}\ 2, \tag{3.25}$$

where $\mathcal{F}$ and $\mathcal{Q}_3$ are expressed in terms of the Berry's connection $\mathcal{A}$ using Eqs. (3.2) and (3.3). The integral is over half of the base space $(1/2)(T^3\times S^1)$, defined such that $(\mathbf{k},\mathbf{r})$ and $(-\mathbf{k},\mathbf{r})$ are never both included. The second term is over the boundary of $(1/2)(T^3\times S^1)$, which is closed under $(\mathbf{k},\mathbf{r}) \rightarrow (-\mathbf{k},\mathbf{r})$. Equation (3.25) must be used with care because the Chern Simons form in the second term depends on the gauge. A different continuous gauge can give a different ν, but due to Eq. (3.24), they must be related by an even integer. Thus, an odd number is distinct.

In addition to satisfying Eq. (3.24), it is essential to use a gauge in which at least $\mathcal{Q}_3$ is continuous on $\partial\frac{1}{2}T^3\times S^1$ (though not necessarily on all of $\frac{1}{2}T^3\times S^1$). This continuous gauge can always be found if the base space is a sphere S^4. However for $T^3\times S^1$, the weak topological invariants can pose an obstruction to finding a continuous gauge. We will show how to work around this difficulty at the end of the following section.

2. Dislocation in a weak topological insulator

Ran, Zhang, and Vishwanath recently studied the problem of a line dislocation in a topological insulator.[75] They found that an insulator with nontrivial weak topological invariants can exhibit topologically protected helical modes at an appropriate line dislocation. In this section we will show that these protected modes are associated with a nontrivial $\mathbb{Z}_2$ invariant in Eq. (3.25). In addition to providing an explicit example for this invariant, this formulation provides additional insight into why protected modes can exist in a weak topological insulator. As argued in Ref. 9 and 12, the weak topological invariants lose their meaning in the presence of disorder. The present considerations show that the helical modes associated with the dislocation are protected by the *strong* topological invariant associated with the line defect. Thus if we start with a perfect crystal and add disorder, then the helical modes remain, even though the crystal is no longer a weak topological insulator. The helical modes remain even if the disorder destroys the crystalline order, so that dislocations become ill defined, *provided* the mobility gap remains finite in the bulk crystal. In this case, the Hamiltonian has a nontrivial winding around the line defect, even though the defect has no obvious structural origin. Thus, the weak topological insulator provides a *route* to realizing the topologically protected line defect. But once present, the line defect is more robust than the weak topological insulator.

To evaluate the $\mathbb{Z}_2$ invariant in Eq. (3.25) for a line dislocation we repeat the analysis in Sec. III A 2. Because of the subtlety with the application of Eq. (3.25) we will first consider the simplest case of a dislocation in a weak topological insulator. Afterward we will discuss the case of a crystal with both weak and strong invariants.

The Bloch functions on a circle surrounding a dislocation are described by Eq. (3.6) and the evaluation of $\mathrm{Tr}[\mathcal{F}\wedge\mathcal{F}]$ proceeds exactly as in Eqs. (3.7)–(3.9). To evaluate the sec-

ond term in Eq. (3.25) we need the Chern-Simons 3 form. One approach is to use Eqs. (3.3) and (3.7). However, this is not continuously defined on $\partial(1/2)(T^3\times S^1)$ because $\mathcal{A}$ has a term $\mathbf{B}\cdot\mathbf{k}ds$ that is discontinuous at the Brillouin zone boundary. An alternative is to write

$$\mathcal{Q}_3 = \mathrm{Tr}[\mathbf{B}\cdot(2\mathcal{A}^0\wedge d\mathbf{k} - [\mathcal{F}^0,\mathbf{a}^p])\wedge ds]. \tag{3.26}$$

From Eq. (3.9) this clearly satisfies $\mathrm{Tr}[\mathcal{F}\wedge\mathcal{F}]=d\mathcal{Q}_3$ and it is defined continuously on $\partial(1/2)(T^3\times S^1)$ as long as $\mathcal{A}^0$ is continuously defined on $\partial(1/2)T^3$. For a weak topological insulator this is always possible, provided $(1/2)T^3$ is defined appropriately. Equation (3.26) differs from Eq. (3.3) by a total derivative.

Combining Eqs. (3.9), (3.25), and (3.26), the terms involving $\mathbf{a}^p$ cancel because $\mathbf{a}^p$ is globally defined. (Note that $\mathbf{a}^p$ is unchanged by a $\mathbf{k}$-dependent—but $\mathbf{r}$-independent—gauge transformation). This cannot be said of the term involving $\mathcal{A}^0$, however, because in a weak topological insulator $\mathcal{A}^0$ is *not* globally defined on $(1/2)T^3$. Performing the trivial integral over s we then find

$$\nu = \frac{1}{2\pi}\mathbf{B}\cdot\mathbf{G}_\nu \bmod 2, \tag{3.27}$$

where

$$\mathbf{G}_\nu = \int_{1/2T^3}\mathrm{Tr}[\mathcal{F}^0]\wedge d\mathbf{k} - \int_{\partial 1/2T^3}\mathrm{Tr}[\mathcal{A}^0]\wedge d\mathbf{k}. \tag{3.28}$$

The simplest case to consider is a weak topological insulator consisting of decoupled layers of 2D quantum spin-Hall insulator stacked with a lattice constant a in the z direction. In this case $\mathcal{F}^0=\mathcal{F}^0(k_x,k_y)$ is independent of k_z so the k_z integral can be performed trivially. This leads to $\mathbf{G}_\nu=(2\pi/a)\nu\hat{\mathbf{z}}$, where

$$\nu = \frac{i}{2\pi}\left[\int_{1/2T^2}\mathrm{Tr}[\mathcal{F}^0] - \int_{\partial 1/2T^2}\mathrm{Tr}[\mathcal{A}^0]\right] \tag{3.29}$$

is the 2D $\mathbb{Z}_2$ topological invariant characterizing the individual layers.

Equation (3.28) also applies to a more general 3D weak topological insulator. A weak topological insulator is characterized by a triad of $\mathbb{Z}_2$ invariants $(\nu_1\nu_2\nu_3)$ that define a mod 2 reciprocal lattice vector[9,12]

$$\mathbf{G}_\nu = \nu_1\mathbf{b}_1 + \nu_2\mathbf{b}_2 + \nu_3\mathbf{b}_3, \tag{3.30}$$

where $\mathbf{b}_i$ are primitive reciprocal lattice vectors corresponding to primitive lattice vectors $\mathbf{a}_i$ (such that $\mathbf{a}_i\cdot\mathbf{b}_j=2\pi\delta_{ij}$). The indices ν_i can be determined by evaluating the 2D invariant in Eq. (3.29) on the time-reversal invariant plane $\mathbf{k}\cdot\mathbf{a}_i=\pi$.

To show that $\mathbf{G}_\nu$ in Eqs. (3.28) and (3.30) are equivalent, consider $\mathbf{G}_\nu\cdot\mathbf{a}_1$ in Eq. (3.28). If we write $\mathbf{k}=x_1\mathbf{b}_1+x_2\mathbf{b}_2+x_3\mathbf{b}_3$, then the integrals over x_2 and x_3 have the form of Eq. (3.29). Since this is quantized, it must be independent of x_1 and will be given by its value at $x_1=1/2$. This then gives $\mathbf{G}_\nu\cdot\mathbf{a}_1=2\pi\nu_1$. A similar analysis of the other components establishes the equivalence. A nontrivial value of Eq. (3.27) is the same as the criterion for the existence of protected helical modes on a dislocation Ran, Zhang, and Vishwanath[75] derived using a different method.

Evaluating Eq. (3.28) in a crystal that is *both* a strong topological insulator and a weak topological insulator (such as $Bi_{1-x}Sb_x$) is problematic because the 2D invariants evaluated on the planes $x_1=0$ and $x_1=1/2$ are necessarily *different* in a strong topological insulator. This arises because a nontrivial strong topological invariant ν_0 is an obstruction to continuously defining $\mathcal{A}^0$ on $\partial(1/2)T^3$ so Eq. (3.29) cannot be evaluated continuously between $x_1=0$ and $x_1=1/2$. From the point of view of the topological classification of the *defect* on $T^3\times S^1$, ν_0 is like a *weak* topological invariant because it a property of T^3 and is independent of the real-space parameter s in S^1. Thus this complication is a manifestation of the fact that topological classification of Hamiltonians on $T^3\times S^1$ has more structure than those on S^4. The problem is not with the existence of the invariant ν on $T^3\times S^1$ but rather with applying the formulas (3.25) and (3.28). The problem can be circumvented with the following trick.

Consider an auxiliary Hamiltonian $\tilde{\mathcal{H}}(\mathbf{k},\mathbf{r})=\mathcal{H}(\mathbf{k},\mathbf{r})\oplus\mathcal{H}_{STI}(\mathbf{k})$, where $\mathcal{H}_{STI}$ is a simple model Hamiltonian for a strong topological insulator such as Eq. (3.13), which can be chosen such that it is a constant independent of $\mathbf{k}$ everywhere except in a small neighborhood close to $\mathbf{k}=0$ where a band inversion occurs. Adding such a Hamiltonian that is independent of $\mathbf{r}$ will have no effect on the topologically protected modes associated with a line defect so we expect the invariant ν to be the same for both $\mathcal{H}(\mathbf{k},\mathbf{r})$ and $\tilde{\mathcal{H}}(\mathbf{k},\mathbf{r})$. If $\mathcal{H}(\mathbf{k},\mathbf{r})$ has a nontrivial strong topological invariant $\nu_0=1$ then $\tilde{\mathcal{H}}(\mathbf{k},\mathbf{r})$ will have $\nu_0=0$, so that Eq. (3.28) can be applied. $\mathbf{G}_\nu$ will then be given by the 2D invariant in Eq. (3.29) evaluated for $\tilde{\mathcal{H}}$, which will be independent of x_1. Since $\mathcal{H}_{STI}(\mathbf{k})$ is $\mathbf{k}$-independent everywhere except a neighborhood of $\mathbf{k}=0$, this will agree with the 2D invariant evaluated for $\mathcal{H}$ at $x_1=1/2$, but not $x_1=0$. It then follows that even in a strong topological insulator the invariant characterizing a line dislocation is given by Eq. (3.27), where $\mathbf{G}_\nu$ is given by Eq. (3.30) in terms of the weak topological invariants.

3. Heterostructure geometries

In principle, it may be possible to realize 1D helical fermions in a 3D system that does not rely on a weak topological insulating state. It is possible to write down a 3D model, analogous to Eq. (3.13) that has bound helical modes. However, it is not clear how to physically implement this model. This model will appear in a more physical context as a BdG theory in the following section.

D. Class DIII: Helical Majorana fermions

Line defects for class DIII are characterized by a $\mathbb{Z}_2$ topological invariant that signals the presence or absence of 1D helical Majorana fermion modes. As in Sec. III B, the BdG Hamiltonian has the same structure as a Bloch Hamiltonian, and the $\mathbb{Z}_2$ invariant can be deduced by "forgetting" the particle-hole symmetry, and treating the problem as if it was a Bloch Hamiltonian in class AII.

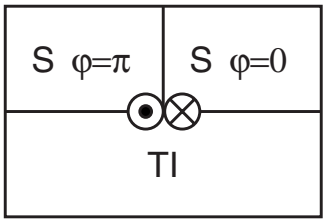

FIG. 6. Helical Majorana fermions at a linear Josephson junction with phase difference π on the surface of a topological insulator.

There are several ways to realize helical Majorana fermions. The simplest is to consider the edge of a 2D time-reversal invariant superconductor or superfluid, or equivalently a dislocation in a layered version of that 2D state. A second is to consider a topological line defect in a 3D class DIII topological superconductor or superfluid. Such line defects are well known in of ^{3}He B (Refs. 41 and 76) and have recently been revisited in Refs. 37 and 77.

Here we will consider a different realization that uses topological insulators and superconductors. Consider a linear junction between two superconductors on the surface of a topological insulator as shown in Fig. 6. In Ref. 48 it was shown that when the phase difference between the superconductors is π there are gapless helical Majorana modes that propagate along the junction. This can be described by an eight-band minimal model that describes a topological insulator surface with a superconducting proximity effect

$$\mathcal{H} = v\tau_z\mu_x\vec{\sigma}\cdot\mathbf{k} + (m + \epsilon|\mathbf{k}|^2)\tau_z\mu_z + \Delta_1\tau_x. \quad (3.31)$$

Here m is the mass describing the band inversion of a topological insulator, as in Eq. (3.22), and Δ_1 is the real part of the superconducting gap parameter. This model has time reversal symmetry with $\Theta = i\sigma_y K$ and particle-hole symmetry with $\Xi = \sigma_y\tau_y K$. The imaginary part of the superconducting gap, $\Delta_2\tau_y$ violates time-reversal symmetry. A line junction along the x direction with phase difference π at the surface of a topological insulator corresponds to the intersection of planes where $m(z)$ and $\Delta_1(y)$ change sign.

The $\mathbb{Z}_2$ invariant characterizing such a line defect is straightforward to evaluate because $[\mathcal{H}, \mu_y\tau_x] = 0$. This extra symmetry allows a "spin Chern number" to be defined, $n_\sigma = (16\pi^2)^{-1}\int \mathrm{Tr}[\mu_y\tau_x\mathcal{F}\wedge\mathcal{F}]$. Since the system decouples into two time reversed versions of Eq. (3.13), $n_\sigma = 1$. By repeating the formulation in Appendix E of the $\mathbb{Z}_2$ invariant ν, it is straightforward to show that this means $\nu = 1$.

The helical modes can be explicitly seen by solving the linear theory, $m = f_z z$, $\Delta_1 = f_y y$, which leads to the harmonic oscillator model studied in Appendix C. In the space of the two zero modes the Hamiltonian has the form

$$\mathcal{H} = vk_x\sigma_x \quad (3.32)$$

and describes 1D helical Majorana fermions.

E. Class C: Chiral Dirac fermions

We finally briefly consider line defects in class C. Class C can be realized when time-reversal symmetry is broken in a superconductor without spin orbit interactions that has even parity singlet pairing. Line defects are characterized by an integer topological invariant that determines the number of chiral Majorana fermion modes associated with the line. As in class D, this may be evaluated by forgetting the particle-hole symmetry and evaluating the corresponding Chern number that would characterize class A. The $2\mathbb{Z}$ in Table II for this case, however, means that the Chern integer computed in this manner is necessarily *even*. This means that there will necessarily be an even number $2n$ of chiral Majorana fermion modes, which may equivalently viewed as n chiral Dirac fermion modes. An example of such a system would be a 2D $d_{x^2-y^2}+id_{xy}$ superconductor,[78] which exhibits chiral Dirac fermion edge states, or equivalently a dislocation in a 3D layered version of that state.

TABLE III. Symmetry classes supporting nontrivial point topological defects and their associated $E=0$ modes.

Symmetry	Topological classes	$E=0$ bound states
AIII	$\mathbb{Z}$	Chiral Dirac
BDI	$\mathbb{Z}$	Chiral Majorana
D	$\mathbb{Z}_2$	Majorana
DIII	$\mathbb{Z}_2$	Majorana Kramers doublet (=Dirac)
CII	$2\mathbb{Z}$	Chiral Majorana Kramers Doublet (=Chiral Dirac)

IV. POINT DEFECTS

Point defects can occur at the end of a 1D system ($\delta=1-0$) or at topological defects in 2D ($\delta=2-1$) or 3D ($\delta=3-2$) systems. From the $\delta=1$ column Table I, it can be seen that there are five symmetry classes that can have topologically nontrivial point defects. These are expected to be associated with protected zero-energy bound states. Table III lists the nontrivial classes, along with the character of the associated zero modes. In this section we will discuss each of these cases.

A. Classes AIII, BDI, and CII: Chiral zero modes

1. Topological invariant and zero modes

Point defects in classes AIII, BDI, and CII are characterized by integer topological invariants. The formula for this integer invariant can be formulated by exploiting the chiral symmetry in each class. In a basis where the chiral symmetry operator is $\Pi = \tau_z$, the Hamiltonian may be written

$$\mathcal{H}(\mathbf{k},\mathbf{r}) = \begin{pmatrix} 0 & q(\mathbf{k},\mathbf{r}) \\ q(\mathbf{k},\mathbf{r})^\dagger & 0 \end{pmatrix}. \quad (4.1)$$

When the Hamiltonian has a flattened eigenvalue spectrum $\mathcal{H}^2 = 1$, $q(\mathbf{k},\mathbf{r})$ is a unitary matrix. For a point defect in d dimensions, the Hamiltonian as a function of d momentum variables and $D=d-1$ position variables is characterized by

the winding number associated with the homotopy $\pi_{2d-1}[U(n\to\infty)]=\mathbb{Z}$, which is given by

$$n=\frac{(d-1)!}{(2d-1)!(2\pi i)^d}\int_{T^d\times S^{d-1}}\mathrm{Tr}[(qdq^\dagger)^{2d-1}]. \quad (4.2)$$

For a Hamiltonian that is built from anticommuting Dirac matrices, $\mathcal{H}(\mathbf{k},\mathbf{r})=\hat{\mathbf{d}}(\mathbf{k},\mathbf{r})\cdot\vec{\gamma}$, this invariant is given simply by the winding degree of the mapping $\hat{\mathbf{d}}(\mathbf{k},\mathbf{r})$ from $T^d\times S^{d-1}$ to S^{2d-1}, which is expressed as an integral of the Jacobian

$$n=\frac{(d-1)!}{2\pi^d}\int_{T^d\times S^{d-1}}d^d\mathbf{k}d^{d-1}\mathbf{r}\frac{\partial\hat{\mathbf{d}}(\mathbf{k},\mathbf{r})}{\partial^d\mathbf{k}\partial^{d-1}\mathbf{r}}. \quad (4.3)$$

In class AIII there are no constraints on $q(\mathbf{k},\mathbf{r})$ other than unitarity so all possible values of n are possible. There are additional constraints for the chiral classes with antiunitary symmetries. As shown in Appendix B, this is simplest to see by analyzing the constraints on the winding degree discussed above. n must be zero in classes CI and DIII. There is no constraint on n in class BDI while n must be even in class CII.

The topological invariant is related to an index that characterizes the chirality of the zero modes

$$n=N_+-N_-, \quad (4.4)$$

where $N_\pm$ are the number of zero modes that are eigenstates of Π with eigenvalue ±1. To see that these zero modes are indeed protected consider $N_+=n>0$ and $N_-=0$. Any term in the Hamiltonian that could shift any of the N_+ degenerate states would have to have a nonzero matrix element connecting states with the same chirality. Such terms are forbidden, though, by the chiral symmetry $\{\mathcal{H},\Pi\}=0$. In the superconducting classes BDI and CII the zero energy states are Majorana bound states. In class CII, however, since time reversal symmetry requires that n must be even, the paired Majorana states can be regarded as zero-energy Dirac fermion states.

In the special case where $\mathcal{H}(\mathbf{k},\mathbf{r})$ has the form of a massive Dirac Hamiltonian, by introducing a suitable regularization for $|\mathbf{k}|\to\infty$ the topological invariant in Eqs. (4.2) and (4.3) can be expressed in a simpler manner as a topological invariant characterizing the mass term. In the following sections we consider this in the three specific cases $d=1,2,3$.

2. Solitons in d=1

The simplest topological zero mode occurs in the Jackiw-Rebbi model,[45] which is closely related to the Su, Schrieffer, and Heeger model.[47] Consider

$$\mathcal{H}(k,x)=vk\sigma_x+m\sigma_y. \quad (4.5)$$

Domain walls where $m(x)$ changes sign as a function of x are associated with the well known zero-energy soliton states.

To analyze the topological class requires a regularization for $|k|\to\infty$. This can either be done with a lattice, as in the Su, Schrieffer, Heeger model or by adding a term $\epsilon k^2\sigma_y$, as in Eq. (3.13) so that $|k|\to\infty$ can be replaced by a single point. In either case, the invariant in Eq. (4.2) changes by 1 when m changes sign.

3. Jackiw-Rossi Model in d=2

Jackiw and Rossi introduced a two-dimensional model that has protected zero modes.[46] The Hamiltonian can be written

$$\mathcal{H}(\mathbf{k},\mathbf{r})=v\vec{\gamma}\cdot\mathbf{k}+\vec{\Gamma}\cdot\vec{\phi}(\mathbf{r}), \quad (4.6)$$

where $\mathbf{k}=(k_x,k_y)$, and (γ_1,γ_2) and (Γ_1,Γ_2) are anticommuting Dirac matrices. They showed that the core of a vortex where $\phi=\phi_1+i\phi_2$ winds by $2\pi n$ is associated with n zero modes that are protected by the chiral symmetry. Viewed as a BdG Hamiltonian, these zero modes are Majorana bound states.

This can be interpreted as a Hamiltonian describing superconductivity in Dirac fermions. In this interpretation the Dirac matrices are expressed as $(\gamma_1,\gamma_2)=\tau_z(\sigma_x,\sigma_y)$ and $(\Gamma_1,\Gamma_2)=(\tau_x,\tau_y)$, where $\vec{\sigma}$ is a Pauli matrix describing spin and $\vec{\tau}$ describes particle-hole space. The superconducting pairing term is $\Delta=\phi_1+i\phi_2$. In this interpretation a vortex violates the physical time-reversal symmetry $\Theta=i\sigma_yK$. However, even in the presence of a vortex this model has a fictitious "time-reversal symmetry" $\tilde{\Theta}=\sigma_x\tau_xK$ which satisfies $\tilde{\Theta}^2=+1$. This symmetry would be violated by a finite chemical potential term $\mu\tau_z$. Combined with particle-hole symmetry $\Xi=\sigma_y\tau_yK$ ($\Xi^2=+1$), $\tilde{\Theta}$ defines the BDI class with chiral symmetry $\Pi=\sigma_z\tau_z$.

Evaluating the topological invariant in Eq. (4.2) again requires a $|\mathbf{k}|\to\infty$ regularization. One possibility is to add $\epsilon|\mathbf{k}|^2\tau_x$ so that $|\mathbf{k}|\to\infty$ can be replaced by a single point. In this case the invariant can be determined by computing the winding degree of $\hat{\mathbf{d}}(\mathbf{k},\mathbf{r})$ on S^3. In the limit $\epsilon\to0$ the $\mathbf{k}$ integral can be performed so that Eq. (4.2) can be expressed as the winding number of the phase of $\phi_1+i\phi_2=|\Delta|e^{i\varphi}$

$$n=\frac{1}{2\pi}\int_{S^1}d\varphi. \quad (4.7)$$

4. Hedgehogs in d=3

In Ref. 53 we introduced a three dimensional model for Majorana bound states that can be interpreted as a theory of a vortex at the interface between a superconductor and a topological insulator. In the special case that the chemical potential is equal to zero, model has the same form as Eq. (4.6), except that now all of the vectors are three dimensional. In the topological insulator model we have $\vec{\gamma}=(\gamma_1,\gamma_2,\gamma_3)=\mu_x\tau_z\vec{\sigma}$ and $\vec{\Gamma}=(\Gamma_1,\Gamma_2,\Gamma_3)=(\mu_z\tau_z,\tau_x,\tau_y)$. $\vec{\tau}$ and $\vec{\sigma}$ are defined as before while $\vec{\mu}$ describes a orbital degree of freedom. The chiral symmetry, $\Pi=\mu_y\tau_z$ is violated if a chemical potential term $\mu\tau_z$ is included.

Following the same steps that led to Eq. (4.7) the invariant Eq. (4.2) is given by the winding number of $\hat{\phi}=\vec{\phi}/|\vec{\phi}|$ on S^2

$$n=\frac{1}{4\pi}\int_{S^2}\hat{\phi}\cdot(d\hat{\phi}\times d\hat{\phi}). \quad (4.8)$$

B. Class D: Majorana bound states

1. Topological invariant

Point defects in class D are characterized by a $\mathbb{Z}_2$ topological invariant that determines the presence or absence of a Majorana bound state associated with the defect. These include the well-known end states in a 1D p-wave superconductor and vortex states in a 2D p_x+ip_y superconductor. In Ref. 53 we considered such zero modes in a three-dimensional BdG theory describing Majorana zero modes in topological insulator structures. Here we develop a unified description of all of these cases.

For a point defect in d dimensions, the Hamiltonian depends on d momentum variables and $D=d-1$ position variables. In Appendix D we show that the $\mathbb{Z}_2$ invariant is given by

$$\nu = \frac{2}{d!}\left(\frac{i}{2\pi}\right)^d \int_{T^d\times S^{d-1}} \mathcal{Q}_{2d-1} \bmod 2, \tag{4.9}$$

where $\mathcal{Q}_{2d-1}$ is the Chern Simons form. The specific cases of interest are

$$\mathcal{Q}_1 = \mathrm{Tr}[\mathcal{A}], \tag{4.10}$$

$$\mathcal{Q}_3 = \mathrm{Tr}\left[\mathcal{A}d\mathcal{A} + \frac{2}{3}\mathcal{A}^3\right], \tag{4.11}$$

$$\mathcal{Q}_5 = \mathrm{Tr}\left[\mathcal{A}(d\mathcal{A})^2 + \frac{3}{2}\mathcal{A}^3 d\mathcal{A} + \frac{3}{5}\mathcal{A}^5\right]. \tag{4.12}$$

It is instructive to see that Eq. (4.9) reduces to Eq. (4.2) in the case in which a system also has particle-hole symmetry. In this case, as detailed in Appendix D it is possible to choose a gauge in which $\mathcal{A}=q^\dagger dq/2$, so that $\mathcal{Q}_{2d-1} \propto (qdq^\dagger)^{2d-1}$.

2. End states in a 1D superconductor

The simplest example of a point defect in a superconductor occurs in Kitaev's model[38] of a one-dimensional p-wave superconductor. This is described by a simple 1D tight binding model for spinless electrons, which includes a nearest-neighbor hopping term $tc_i^\dagger c_{i+1}$+H.c. and a nearest-neighbor p-wave pairing term $\Delta c_i c_{i+1}$+H.c.. The Bogoliubov de Gennes Hamiltonian can then be written as

$$\mathcal{H}(k) = (t\cos k - \mu)\tau_z + \Delta \sin k \tau_x. \tag{4.13}$$

This model exhibits a weak pairing phase for $|\mu|<t$ and a strong pairing phase for $|\mu|>t$. The weak pairing phase will have zero-energy Majorana states at its ends.

The topological invariant in Eq. (4.9) can be easily evaluated. We find $\mathcal{A}=d\theta/2$, where θ is the polar angle of $\mathbf{d}(k)=(t\cos k-\mu,\Delta \sin k)$. It follows that for $|\mu|<t$, the topological invariant is $\nu=1$ mod 2.

3. Vortex in a 2D topological superconductor

In two dimensions, a Majorana bound state occurs at a vortex in a topological superconductor. This can be easily seen by considering the edge states of the topological superconductor in the presence of a hole.[39] Particle-hole symmetry requires that the quantized edge states come in pairs. When the flux is an odd multiple of $h/2e$, the edge states are quantized such that a zero mode is present. In this section we will evaluate the topological invariant in Eq. (4.9) associated with a loop surrounding the vortex.

We begin with the class D BdG Hamiltonian $\mathcal{H}_p^0(k_x,k_y)$ characterizing the topological superconductor when the superconducting phase is zero. We include the subscript p to denote the first Chern number that classifies the topological superconductor. We can then introduce a nonzero superconducting phase by a gauge transformation

$$\mathcal{H}_p(\mathbf{k},\varphi) = e^{-i\varphi\tau_z/2}\mathcal{H}_p^0(\mathbf{k})e^{i\varphi\tau_z/2}, \tag{4.14}$$

where τ_z operates in the Nambu particle-hole space. We now wish to evaluate Eq. (4.9) for this Hamiltonian when phase $\varphi(s)$ winds around a vortex. There is, however, a difficulty because the Chern Simons formula requires a gauge that is continuous throughout the entire base space $T^2\times S^1$. The nonzero Chern number p characterizing $\mathcal{H}_p^0(\mathbf{k})$ is an obstruction to constructing such a gauge. A similar problem arose in Sec. III C 2, when we discussed a line dislocation in a weak topological superconductor. We can adapt the trick we used there to get around the present problem. We thus double the Hilbert space to include two copies of our Hamiltonian, one with Chern number p and one with Chern number $-p$

$$\tilde{\mathcal{H}}^0(\mathbf{k}) = \begin{pmatrix} \mathcal{H}_p^0(\mathbf{k}) & 0 \\ 0 & \mathcal{H}_{-p}^0(\mathbf{k}) \end{pmatrix}. \tag{4.15}$$

We then put the vortex in only the $+p$ component

$$\tilde{\mathcal{H}}(\mathbf{k},\varphi) = e^{-i\varphi q}\tilde{\mathcal{H}}^0(\mathbf{k})e^{i\varphi q}, \tag{4.16}$$

where

$$q = \frac{1+\tau_z}{2}\begin{pmatrix} 1 & 0 \\ 0 & 0 \end{pmatrix}. \tag{4.17}$$

We added an extra phase factor by replacing τ_z by $1+\tau_z$ in order to make $e^{i\varphi q}$ periodic under $\varphi\to\varphi+2\pi$.

Since the Chern number characterizing $\tilde{\mathcal{H}}^0(\mathbf{k})$ is zero, there exists a continuous gauge

$$|\tilde{u}_i(\mathbf{k},\varphi)\rangle = e^{i\varphi q}|\tilde{u}_i^0(\mathbf{k})\rangle, \tag{4.18}$$

which allows us to evaluate the Chern-Simons integral. The Berry's connection $\tilde{\mathcal{A}}_{ij}=\langle\tilde{u}_i|d\tilde{u}_j\rangle$ is given by

$$\tilde{\mathcal{A}} = \tilde{\mathcal{A}}^0 + iQd\varphi, \tag{4.19}$$

where $\tilde{\mathcal{A}}^0(\mathbf{k})$ is the connection describing $\tilde{\mathcal{H}}^0(\mathbf{k})$ and $Q_{ij}(\mathbf{k})=\langle\tilde{u}_i^0(\mathbf{k})|q|\tilde{u}_j^0(\mathbf{k})\rangle$. Inserting this into Eq. (4.11) and rearranging terms we find

$$\mathcal{Q}_3 = \mathrm{Tr}[2Q\tilde{\mathcal{F}}^0 - d(Q\tilde{\mathcal{A}}^0)]\wedge d\varphi, \tag{4.20}$$

where $\tilde{\mathcal{F}}^0=d\tilde{\mathcal{A}}^0+\tilde{\mathcal{A}}^0\wedge\tilde{\mathcal{A}}^0$. Since the second term is a total derivative it can be discarded. For the first term there are two contributions from the 1 and the τ_z in Eq. (4.17). Upon inte-

grating over $\mathbf{k}$, the τ_z term can be shown to vanish as a consequence of particle-hole symmetry. The 1 term simply projects out the Berry curvature of the original Hamiltonian $\mathcal{H}_p^0(\mathbf{k})$ so that

$$\mathcal{Q}_3 = \mathrm{Tr}[\mathcal{F}^0] \wedge d\varphi. \tag{4.21}$$

It follows from Eq. (4.9) that the $\mathbb{Z}_2$ invariant characterizing the vortex is

$$\nu = pm \bmod 2, \tag{4.22}$$

where p is the Chern number characterizing the topological superconductor and m is the phase winding number associated with the vortex.

It is also instructive to consider this invariant in the context of the simple two-band model introduced by Read and Green.[39] This can be written as a simple tight-binding model

$$\mathcal{H}^0(k_x,k_y) = [t(\cos k_x + \cos k_y) - \mu]\tau_z + \Delta(\sin k_x \tau_x + \sin k_y \tau_y), \tag{4.23}$$

where the superconducting order parameter Δ is real. As in Eq. (4.13), this model exhibits weak and strong pairing phases for $|\mu| < t$ and $|\mu| > t$. These are distinguished by the Chern invariant, which in turn is related to the winding number on S^2 of the unit vector $\hat{\mathbf{d}}(\mathbf{k})$, where $\vec{d}(\mathbf{k})$ are the coefficients of $\vec{\tau}$ in Eq. (4.23). A nonzero superconducting phase is again introduced by rotating about τ_z as in Eq. (4.14). Here we wish to show that in this two band model the $\mathbb{Z}_2$ invariant ν can be understood from a geometrical point of view.

The Z_2 invariant characterizing a vortex can be understood in terms of the topology of the maps $\hat{\mathbf{d}}(k_x,k_y,\phi)$. from $T^2 \times S^1$ to S^2. These maps were first classified by Pontrjagin[79] and have also appeared in other physical contexts.[53,80,81] Without losing generality, we can reduce the torus T^2 to a sphere S^2 so the mappings are $S^2 \times S^1 \to S^2$. When for fixed ϕ $\hat{\mathbf{d}}(k_x,k_y,\phi)$ has an S^2 winding number of $\pm p$, the topological classification is $\mathbb{Z}_{2p}$. In the case of interest, $p=1$, so there are two classes.

This $\mathbb{Z}_2$ Pontrjagin invariant can be understood pictorially by considering inverse image paths in $(\mathbf{k},\phi)$ space, which map to two specific points on S^2. These correspond to 1D curves in $S^2 \times S^1$. Figure 7 shows three examples of such curves. The inner sphere corresponds to $\phi=0$ while the outer sphere corresponds to $\phi=2\pi$. Since $p=1$, for every point on S^2 the inverse image path is a single curve connecting the inner and outer spheres. The key point is to examine the linking properties of these curves. The $\mathbb{Z}_2$ invariant describes the number of twists in a pair of inverse image paths, which is 1 in (a), 2 in (b), and 0 in (c). The configuration in (b) can be continuously deformed into that in (c) by dragging the paths around the inner sphere. This can be verified by a simple demonstration using your belt. The twist in (a), however, cannot be undone. The number of twists thus defines the $\mathbb{Z}_2$ Pontrjagin invariant.

4. Superconductor heterostructures

Finally, in three dimensions, a nontrivial point defect can occur at a superconductor heterostructure. An example is a vortex in the superconducting state at the interface between a superconductor and a topological insulator. As shown in Ref. 53, this can be described by the simple Hamiltonian

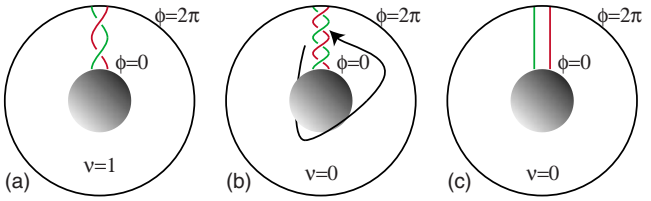

FIG. 7. (Color online) Visualization of the $\mathbb{Z}_2$ Pontrjagin invariant characterizing maps from $(\mathbf{k},\phi) \in S^2 \times S^1$ to S^2 when the winding degree for each ϕ is 1. The inner sphere corresponds to $\mathbf{k}$ at $\phi=0$ while the outer sphere is $\phi=2\pi$. The lines depict inverse images of two specific points on S^2, which are lines connecting the inner and outer spheres. In (a) they have one twist, which cannot be eliminated. The double twist in (b) can be unwound by smoothly dragging the paths around the sphere to arrive at (c), which has no twist.

$$\mathcal{H} = v\tau_z\mu_x\vec{\sigma}\cdot\mathbf{k} - \mu\tau_z + (m + \epsilon|\mathbf{k}|^2)\tau_z\mu_z + \Delta_1\tau_x + \Delta_2\tau_y. \tag{4.24}$$

Here m is a mass which distinguishes a topological insulator from a trivial insulator, and $\Delta=\Delta_1+i\Delta_2$ is a superconducting order parameter. For $\mu=0$, this Hamiltonian has the form of the three dimensional version of Eq. (4.6) discussed in Sec. IV A 4, where the mass term is characterized by the vector $\vec{\phi}=(m,\Delta_1,\Delta_2)$. A vortex in Δ at the interface where m changes sign then corresponds to a hedgehog singularity in $\vec{\phi}$. From Eq. (4.3), it can be seen that the class BDI $\mathbb{Z}$ invariant is $n=1$. This then establishes that the class D $\mathbb{Z}$ invariant is $\nu=1$. The $\mathbb{Z}_2$ survives when a nonzero chemical potential reduces the symmetry from class BDI to class D.

C. Class DIII: Majorana doublets

Point defects in class DIII are characterized by a $\mathbb{Z}_2$ topological invariant. These are associated with zero modes, but unlike class D, the zero modes are required by Kramers theorem to be doubly degenerate. The zero modes thus form a Majorana doublet, which is equivalent to a single Dirac fermion.

In Table I, Class DIII, $\delta=1$ is an entry that is similar to Class AII, $\delta=2$. The $\mathbb{Z}_2$ for DIII invariant bears a resemblance to the invariant for AII, which is a generalization of the $\mathbb{Z}_2$ invariant characterizing the 2D quantum spin-Hall insulator. In Appendix B we will establish a formula that employs the same gauge constraint

$$w(\mathbf{k},\mathbf{r}) = w_0, \tag{4.25}$$

where w_0 is a constant independent of $\mathbf{k}$ and $\mathbf{r}$. $w(\mathbf{k},\mathbf{r})$ relates the time-reversed states at $\mathbf{k}$ and $-\mathbf{k}$ and is given by Eq. (3.23). *Provided* we choose a gauge that satisfies this constraint, the $\mathbb{Z}_2$ invariant is given by

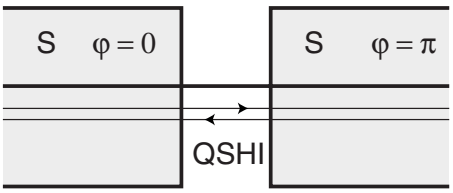

FIG. 8. A Josephson junction in proximity with the helical edge states of a quantum spin-Hall insulator. When the phase difference is π, there is a zero energy Majorana doublet at the junction.

$$\tilde{\nu} = \frac{1}{d!}\left(\frac{i}{2\pi}\right)^d \int_{T^d \times S^{d-1}} \mathcal{Q}_{2d-1} \bmod 2. \tag{4.26}$$

This formula is almost identical to the formula for a point defect in class D but they differ by an important factor of two. Due to the combination of time-reversal and particle-hole symmetries the Chern-Simons integral in Eq. (4.26) is guaranteed to be an integer but the integer is not gauge invariant. When the time-reversal constraint is satisfied, the parity $\tilde{\nu}$ is gauge invariant. It then follows that the class D invariant in Eq. (4.9), $\nu = 0 \bmod 2$.

In the special case $d=1$ there is a formula that does not rely on the gauge constraint, though it still requires a globally defined gauge. It is related to the similar "fixed-point" formula for the invariant for the 2D quantum spin-Hall insulator,[73] and has recently been employed by Qi, Hughes, and Zhang[82] to classify one-dimensional time-reversal invariant superconductors. In class DIII, it is possible to choose a basis in which the time-reversal and particle-hole operators are given by $\Theta = \tau_y K$ and $\Xi = \tau_x K$ so that the chiral operator is $\Pi = \tau_z$. In this basis, the Hamiltonian has the form (4.1), where $q(\mathbf{k},\mathbf{r}) \to q(k)$ satisfies $q(-k) = -q(k)^T$. Thus, $\mathrm{Pf}[q(k)]$ is defined for the time-reversal invariant points $k=0$ and $k=\pi$. $q(k)$ is related to $w(k)$ because in a particular gauge it is possible to choose $w(k) = q(k)/\sqrt{|\mathrm{Det}[q(k)]|}$. The $\mathbb{Z}_2$ invariant is then given by

$$(-1)^{\tilde{\nu}} = \frac{\mathrm{Pf}[q(\pi)]}{\mathrm{Pf}[q(0)]} \frac{\sqrt{\mathrm{Det}[q(0)]}}{\sqrt{\mathrm{Det}[q(\pi)]}}, \tag{4.27}$$

where the branch $\sqrt{\mathrm{Det}[q(k)]}$ is chosen continuously between $k=0$ and $k=\pi$. The equivalence of Eqs. (4.26) and (4.27) for $d=1$ is demonstrated in Appendix A. Unlike Eq. (4.26), however, the fixed-point formula (4.27) does not have a natural generalization for $d>1$.

Majorana doublets can occur at topological defects in time-reversal invariant topological superconductors, or in Helium 3B. Here we consider a different configuration at a Josephson junction at the edge of a quantum spin-Hall insulator (Fig. 8). When the phase difference across the Josephson junction is π, it was shown in Refs. 38 and 83 that there is a level crossing in the Andreev bound states at the junction. This corresponds precisely to a Majorana doublet.

This can be described by the simple continuum 1D theory introduced in Ref. 83

$$\mathcal{H} = vk\tau_z\sigma_z + \Delta_1\tau_x. \tag{4.28}$$

Here σ_z describes the spin of the quantum spin-Hall edge state and Δ_1 is the real superconducting order parameter. This model has particle-hole symmetry $\Xi = \sigma_y\tau_y K$ and time-reversal symmetry $\Theta = i\sigma_y K$ and is in class DIII. A π junction corresponds to a domain wall where Δ_1 changes sign. Following appendix C, it is straightforward to see that this will involve a degenerate pair of zero modes indexed by the spin σ_z and chirality τ_y constrained by $\tau_y\sigma_z = -1$.

The Hamiltonian (4.28) should be viewed as a low-energy theory describing the edge of a 2D quantum spin-Hall insulator. Nonetheless, we may describe a domain wall where Δ_1 changes sign using an effective one dimensional theory by introducing a regularization replacing Δ_1 by $\Delta_1 + \epsilon k^2$. This regularization will not affect the topological structure of a domain wall, where Δ_1 changes sign. A topologically equivalent lattice version of the theory then has the form

$$\mathcal{H} = t \sin k \tau_z\sigma_z + [\Delta_1 + u(1-\cos k)]\tau_x. \tag{4.29}$$

where we assume $|\Delta_1| < 2u$.

The topological invariant can be evaluated using either Eq. (4.26) or (4.27). To use Eq. (4.26), note that Eq. (4.29) has exactly the same form as two copies (distinguished by $\sigma_z = \pm 1$) of Eq. (4.13). The evaluation of Eq. (4.26) then proceeds along the same lines. It is straightforward to check that in a basis where the time-reversal constraint in Eq. (4.25) is satisfied (this fixes the relative phases of the $\sigma_z = \pm 1$ states), $\mathcal{A} = d\theta$, where θ is the polar angle of $\mathbf{d}(k) = [t \sin k, \Delta_1 + u(1-\cos k)]$. It follows that a defect where Δ_1 changes sign has $\tilde{\nu} = 1$.

To use Eq. (4.27), we transform to a basis in which $\Theta = \tau_y K$, $\Xi = \tau_x K$, and $\Pi = \tau_z$. This is accomplished by the unitary transformation $U = \exp[i(\pi/4)\sigma_y\tau_z]\exp[i(\pi/4)\tau_x]$. Then, $\mathcal{H}$ has the form of Eq. (3.13) with $q(k) = -i\{t \sin k\sigma_z + [\Delta_1 + u(1-\cos k)]\sigma_y\}$. It follows that $\det[q(k)]$ is real and positive for all k. Moreover, $\mathrm{Pf}[q(0)]/\sqrt{\det[q(0)]} = \mathrm{sgn}[\Delta_1]$ while $\mathrm{Pf}[q(\pi)]/\sqrt{\det[q(\pi)]} = 1$. Again, a defect where Δ_1 changes sign has $\tilde{\nu} = 1$.

V. ADIABATIC PUMPS

In this section we will consider time-dependent Hamiltonians $\mathcal{H}(\mathbf{k},\mathbf{r},t)$, where in additional to having adiabatic spatial variation $\mathbf{r}$ there is a cyclic adiabatic temporal variation parameterized by t. We will focus on pointlike spatial defects, in which the dimensions of $\mathbf{k}$ and $\mathbf{r}$ are related by $d - D = 1$.

Adiabatic cycles in which $\mathcal{H}(\mathbf{k},\mathbf{r},t=T) = \mathcal{H}(\mathbf{k},\mathbf{r},t=0)$ can be classified topologically by considering t to be an additional "spacelike" variable, defining $\tilde{D} = D+1$. Such cycles will be classified by the $\delta=0$ column of Table I. Topologically nontrivial cycles correspond to adiabatic pumps. Table IV shows the symmetry classes which host nontrivial pumping cycles, along with the character of the adiabatic pump. There are two general cases. Classes A, AI, and AII define a charge pump, where after one cycle an integer number of charges is transported toward or away from the point defect.

TABLE IV. Symmetry classes that support nontrivial charge or fermion parity pumping cycles.

Symmetry	Topological classes	Adiabatic Pump
A	$\mathbb{Z}$	Charge
AI	$\mathbb{Z}$	Charge
BDI	$\mathbb{Z}_2$	Fermion parity
D	$\mathbb{Z}_2$	Fermion parity
AII	$2\mathbb{Z}$	Charge Kramers doublet

Classes BDI and D define a fermion parity pump. We will discuss these two cases separately.

We note in passing that the $\delta=0$ column of Table I also applies to topological *textures*, for which $d=D$. For example, a spatially dependent three-dimensional band structure $\mathcal{H}(\mathbf{k},\mathbf{r})$ can have topological textures analogous to Skyrmions in a 2D magnet. Such textures have recently been analyzed by Ran, Hosur, and Vishwanath[84] for the case of class D, where they showed that the $\mathbb{Z}_2$ invariant characterizing the texture corresponds to the fermion parity associated with the texture. Thus, nontrivial textures are fermions.

A. Classes A, AI, and AII: Thouless charge pumps

The integer topological invariant characterizing a pumping cycle in class A is simply the Chern number characterizing the Hamiltonian $\mathcal{H}(\mathbf{k},\mathbf{r},t)$.[60,61] Imposing time-reversal symmetry has only a minor effect on this. For $\Theta^2=-1$ (Class AII), an odd Chern number violates time-reversal symmetry so that only even Chern numbers are allowed. This means that the pumping cycle can only pump Kramers pairs of electrons. For $\Theta^2=+1$ (Class AI) all Chern numbers are consistent with time-reversal symmetry.

The simplest charge pump is the 1D model introduced by Thouless.[60] A continuum version of this model can be written in the form

$$\mathcal{H}(k,t)=vk\sigma_z+[m_1(t)+\epsilon k^2]\sigma_x+m_2(t)\sigma_y. \tag{5.1}$$

When the masses undergo a cycle such that the phase of m_1+im_2 a single electron is transmitted down the wire. In this case, $\mathcal{H}(k,t)$ has a nonzero first Chern number. The change in the charge associated with a point in a 1D system is given by the difference in the Chern numbers associated with either side of the point. Thus, after a cycle a charge e accumulates at the end of a Thouless pump.

A two-dimensional version of the charge pump can be developed based on Laughlin's argument[85] for the integer quantum-Hall effect. Consider a 2D $\nu=1$ integer quantum-Hall state and change the magnetic flux threading a hole from 0 to h/e. In the process, a charge e is pumped to the edge states surrounding the hole. This pumping process can be characterized by the second Chern number characterizing the 2D Hamiltonian $\mathcal{H}(k_x,k_y,\theta,t)$, where θ parameterizes a circle surrounding the hole. A similar pump in 3D can be considered and is characterized by the third Chern number.

B. Class D, BDI: Fermion parity pump

Adiabatic cycles of point defects in class D and BDI are characterized by a $\mathbb{Z}_2$ topological invariant. In this section we will argue that a nontrivial pumping cycle transfers a unit of fermion parity to the point defect. This is intimately related to the Ising non-Abelian statistics associated with defects supporting Majorana bound states.

Like the point defect in class DIII ($\delta=1$), the temporal pump ($\delta=0$) in class D occupies an entry in Table I similar to the line defect ($\delta=2$) in class AII so we expect a formula that is similar to the formula for the 2D quantum spin-Hall insulator. This is indeed the case, though the situation is slightly more complicated. The Hamiltonian $\mathcal{H}(\mathbf{k},\mathbf{r},t)$ is defined on a base space $T^d\times S^{d-1}\times S^1$. In Appendix F we will show that the invariant can be written in a form that resembles Eq. (3.25)

$$\nu=\frac{i^d}{d!(2\pi)^d}\left[\int_{\mathcal{T}_{1/2}}\mathrm{Tr}(\mathcal{F}^d)-\oint_{\partial\mathcal{T}_{1/2}}\mathcal{Q}_{2d-1}\right]\mathrm{mod}\ 2, \tag{5.2}$$

where $\mathcal{T}_{1/2}$ is half of the base manifold, say, $k_1\in[0,\pi]$, and the Chern-Simons form $\mathcal{Q}_{2d-1}$ is generated by a continuous valence frame $u_v(\mathbf{k},\mathbf{r},t)|_{k_1=0,\pi}$ that obeys certain particle-hole gauge constraint. This is more subtle than the time-reversal gauge condition in Eq. (3.24) for line defects in AII and point defects in DIII. Unlike Eq. (3.24), we do not have a computational way of checking whether or not a given frame satisfies the constraint. Nevertheless, it can be defined, and in certain simple examples, the particle-hole constraint is automatically satisfied.

The origin of the difficulty is that unlike time-reversal symmetry, particle-hole symmetry connects the conduction and valence bands. The gauge constraint therefore involves both. Valence and conduction frames can be combined to form a unitary matrix

$$G_{\mathbf{k},\mathbf{r},t}=\begin{pmatrix} | & | \\ u_v(\mathbf{k},\mathbf{r},t) & u_c(\mathbf{k},\mathbf{r},t) \\ | & | \end{pmatrix}\in U(2n). \tag{5.3}$$

The orthogonality of conduction and valence band states implies that

$$G^\dagger_{\mathbf{k},\mathbf{r},t}\Xi G_{-\mathbf{k},\mathbf{r},t}=0. \tag{5.4}$$

In general, we call a frame $G:\partial\mathcal{T}_{1/2}\to U(2n)$ particle-hole trivial if it can continuously be deformed to a constant *while satisfying Eq. (5.4) throughout the deformation*. The Chern Simons term in Eq. (5.2) requires a gauge that is built from the valence-band part of a particle-hole trivial frame.

Though the subtlety of the gauge condition makes a general computation of the invariant difficult, it is possible to understand the invariant in the context of specific models. Consider, a theory based on a point defect in the d-dimensional version of Eq. (4.6)

$$\mathcal{H}(\mathbf{k},\mathbf{r},t) = v\,\vec{\gamma}\cdot\mathbf{k} + \vec{\Gamma}\cdot\vec{\phi}(\mathbf{r},t). \tag{5.5}$$

Here $\vec{\Gamma}$ and $\vec{\gamma}$ are $2^d \times 2^d$ Dirac matrices, and we suppose that for fixed t, the d-dimensional mass vector $\vec{\phi}(\mathbf{r},t)$ has a point topological defect at $\mathbf{r}_0(t)$. If Ref. 53 we argued that adiabatic cycles for such point defects are classified by a Pontrjagin invariant similar to that discussed in Sec. IV B 3. This may also be understood in terms of the rotation of the "orientation" of the defect. Near the defect, suppose $\vec{\phi}(\mathbf{r},t)=O(t)[\mathbf{r}-\mathbf{r}_0(t)]$, where $O(t)$ is a time-dependent $O(d)$ rotation. In the course of the cycle, the orientation of the topological defect, characterized by $O(t)$ goes through a cycle. Since for $d\geq 3$, $\pi_1[O(d)]=\mathbb{Z}_2$, there are two classes of cycles. As shown in Ref. 53, the nontrivial cycle, which corresponds to a 2π rotation changes the sign of the Majorana fermion wave function associated with the topological defect. We will argue below that this corresponds to a change in the local fermion parity in the vicinity of the defect. For $d=2$, $\pi_1[O(2)]=\mathbb{Z}$. However, the change in the sign of the Majorana bound state is given by the parity of the $O(2)$ winding number. In theories with more bands, it is only this parity that is topologically robust.

In $d=1$, the single Γ matrix in the two-band model does not allow for continuous rotations. Consider instead Kitaev's model[38] for a 1D topological superconductor with at time-dependent phase

$$\mathcal{H}(k,t) = (t\cos k - \mu)\tau_z + \Delta_1(t)\sin k\tau_x + \Delta_2(t)\sin k\tau_y. \tag{5.6}$$

In this case it is possible to apply the formula (5.2) because on the boundary $\partial\mathcal{T}$, which is $k=0$ or $k=\pi$ the Hamiltonian is independent of t, so that the gauge condition in Eq. (5.4) is automatically satisfied. Moreover, the second term in Eq. (5.2) involving the Chern Simons integral is equal to zero so that the invariant is simply the integral of $\mathcal{F}(x,t)$ over $\mathcal{T}_{1/2}$. It is straightforward to check that this gives $\nu=1$.

In order to see why this corresponds to a pump for fermion parity, suppose a topological superconductor is broken in two places, as shown in Fig. 9. At the ends where the superconductor is cut there will be Majorana bound states. The pair of bound states associated with each cut defines two quantum states which differ by the *parity* of the number of electrons. If the two ends are weakly coupled by electron tunneling then the pair of states will split. Now consider advancing the phase of the central superconductor by 2π. As shown in Refs. 38 and 83, the states interchange as depicted in Fig. 9. The level crossing that occurs at π phase difference is protected by the conservation of fermion parity. Thus, at the end of the cycle, one unit of fermion parity has been transmitted from one circled region to the other. The pumping of fermion parity also applies to adiabatic cycles of point defects in higher dimensions and is deeply connected with the Ising non-Abelian statistics associated with those defects.[53]

VI. CONCLUSION

In this paper we developed a unified framework for classifying topological defects in insulators and superconductors

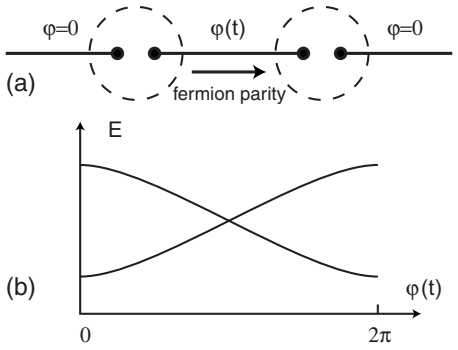

FIG. 9. A one-dimensional fermion parity pump based on a 1D topological superconductor, which has Majorana states at its ends. When the phase of the central superconductor is advanced by 2π the fermion parity associated with the pairs of Majorana states inside each circle changes. Thus fermion parity has been pumped from one circle to the other. (b) shows the evolution of the energy levels associated with a weakly coupled pair of Majorana states as a function of phase. The level crossing at $\phi=\pi$ is protected by the local conservation of fermion parity.

by considering Bloch/BdG Hamiltonians that vary adiabatically with spatial (and/or temporal) parameters. This led to a generalization of the bulk-boundary correspondence, which identifies protected gapless fermion excitations with topological invariants characterizing the defect. This leads to a number of additional questions to be addressed in future work.

The generalized bulk-boundary correspondence has the flavor of a mathematical index theorem, which relates an analytic index that characterizes the zero modes of a system to a topological index. It would be interesting to see a more general formulation of this relation[86,87] that applies to the classes without chiral symmetry that have $\mathbb{Z}_2$ invariants and goes beyond the adiabatic approximation we used in this paper. Though the structure of the gapless modes associated with defects make it clear that such states are robust in the presence of disorder and interactions, it would be desirable to have a more general formulation of the topological invariants characterizing a defect that can be applied to interacting and/or disordered problems.

An important lesson we have learned is that topologically protected modes can occur in a context somewhat more general than simply boundary modes. This expands the possibilities for engineering these states in physical systems. It is thus an important future direction to explore the possibilities for heterostructures that realize topologically protected modes. The simplest version of this would be to engineer protected chiral fermion modes using a magnetic topological insulator. The perfect electrical transport in such states could have far reaching implications at both the fundamental and practical level. In addition, it is worth considering the expanded possibilities for realizing Majorana bound states in superconductor heterostructures, which could have implications for quantum computing.

Finally, it will be interesting to generalize these topological considerations to describe inherently correlated states, such as the Laughlin state. Could a *fractional* quantum-Hall edge state arise as a topological line defect in a 3D system?

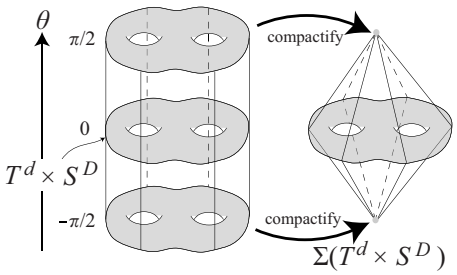

FIG. 10. Suspension $\Sigma(T^d \times S^D)$. The top and bottom of the cylinder $\Sigma(T^d \times S^D) \times [-\pi/2, \pi/2]$ are identified to two points.

Understanding the topological invariants that would characterize such a defect would lead to a deeper understanding of topological states of matter.

ACKNOWLEDGMENTS

We thank Claudio Chamon, Liang Fu, Takahiro Fukui, and Roman Jackiw for helpful discussions. This work was supported by NSF under Grant No. DMR-0906175. We thank R. Jackiw for asking the question that inspired the calculation that led to Eq. (4.22).

APPENDIX A: PERIODICITY IN SYMMETRY AND DIMENSION

In this appendix we will establish the relations in Eqs. (2.5) and (2.6) between the K groups in different position-momentum dimensions (D,d) and different symmetry classes s. We will do so by starting with an arbitrary Hamiltonian in $K_{\mathbb{F}}(s;D,d)$ and then explicitly constructing new Hamiltonians in one higher position or momentum dimension, which have a symmetry either added or removed. The new Hamiltonians will then belong to $K_{\mathbb{F}}(s+1;D,d+1)$ or $K_{\mathbb{F}}(s-1;D+1,d)$. The first step is to identify the mappings and show they preserve the group structure. This defines group homomorphisms relating the K groups. The next step is to show they are *isomporphisms* by showing that the maps have an inverse, up to homotopic equivalence.

1. Hamiltonian mappings

There are two classes of mappings: those that add symmetries and those that remove symmetries. These need to be considered separately.

We consider first the symmetry removing mappings that send a Hamiltonian $\mathcal{H}_c$ with chiral symmetry to a Hamiltonian $\mathcal{H}_{nc}$ without chiral symmetry. Suppose $\{\mathcal{H}_c(\mathbf{k},\mathbf{r}),\Pi\}=0$, where Π is the chiral operator. Then define

$$\mathcal{H}_{nc}(\mathbf{k},\mathbf{r},\theta) = \cos\,\theta\mathcal{H}_c(\mathbf{k},\mathbf{r}) + \sin\,\theta\Pi \tag{A1}$$

for $-\pi/2 \le \theta \le \pi/2$. This has the property that at $\theta = \pm\pi/2$ the new Hamiltonian is $\pm\Pi$, independent of $\mathbf{k}$ and $\mathbf{r}$. Thus, at each of these points we may consider the base space $T^d \times S^D$ defined by $\mathbf{k}$ and $\mathbf{r}$ to be contracted to a point. The new Hamiltonian is then defined on the *suspension* $\Sigma(T^d \times S^D)$ of the original base space (see Fig. 10). If we treat the original base space as a $d+D$-dimensional sphere, then the suspension is a $d+D+1$-dimensional sphere.

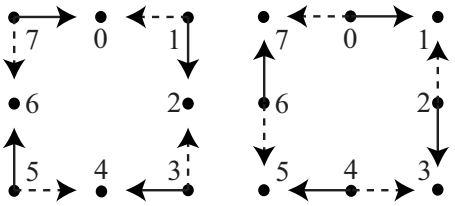

FIG. 11. Hamiltonian mappings in Eqs. (A1) and (A3) are drawn on the left and right clocks, respectively. Solid (dotted) arrows represent addition of one momentum (spatial) dimension.

Without loss of generality we assume $\mathcal{H}_c$ is flattened so that $\mathcal{H}_c^2=1$. Since $\{\mathcal{H}_c,\Pi\}=0$ it follows that $\mathcal{H}_{nc}^2=1$ as well. The second term in Eq. (A1) violates the chiral symmetry. Thus, if $\mathcal{H}_c$ belongs to the complex class AIII (with no antiunitary symmetries), then $\mathcal{H}_{nc}$ belongs to class A. Equation (A1) thus provides a mapping from class AIII to class A.

For the real classes, which have antiunitary symmetries, the second term will violate either particle-hole symmetry or time-reversal symmetry, depending on whether θ is a momentum or position-type variable (odd or even under Θ and Ξ). This will lead to a new nonchiral symmetry class related to the original class by either a clockwise or counterclockwise turn on the symmetry clock (Fig. 11). To determine which it is, note that if we require $[\Theta,\Xi]=0$ then $(\Theta\Xi)^2 = \Theta^2\Xi^2 = (-1)^{(s-1)/2}$. The unitary chiral symmetry operator (satisfying $\Pi^2=1$) can then be written

$$\Pi = i^{(s-1)/2}\Theta\Xi. \tag{A2}$$

It follows that if θ is momentumlike, then time-reversal symmetry is violated when $s=1$ mod 4, while particle hole is violated when $s=3$ mod 4. This corresponds to corresponds to a clockwise rotation on the symmetry clock, $s \to s+1$. If θ is position like then $s \to s-1$.

We next build a chiral Hamiltonian from a nonchiral one by adding a symmetry. This is accomplished by doubling the number of bands in a manner similar to the doubling employed in the Bogoliubov de Gennes description of a superconductor. We thus write

$$\mathcal{H}_c(\mathbf{k},\mathbf{r},\theta) = \cos\,\theta\mathcal{H}_{nc}(\mathbf{k},\mathbf{r}) \otimes \tau_z + \sin\,\theta\mathbb{1} \otimes \tau_a, \tag{A3}$$

where $a=x$ or y. Here $\vec{\tau}$ are Pauli matrices that act on the doubled degree of freedom. As in Eqs. (A1), Eq. (A3) gives a new Hamiltonian defined on a base space that is the suspension of the original base space. If $\mathcal{H}_{nc}^2=1$ it follows that $\mathcal{H}_c^2=1$ so the energy gap is preserved. It is also clear that the new Hamiltonian has a chiral symmetry because it anticommutes with $\Pi = i\tau_z\tau_a$. Thus, if $\mathcal{H}_{nc}$ is in class A, then $\mathcal{H}_c$ is in class AIII.

For the real-symmetry classes $a=x$ or y must be chosen so that the second term in Eq. (A3) preserves the original antiunitary symmetry of $\mathcal{H}_{nc}$. This depends on the original antiunitary symmetry and whether θ is chosen to be a momentum or a position variable. For example, if $\mathcal{H}_{nc}$ has time-reversal symmetry, Θ, and θ is a momentum (position) variable, then we require $a=y$ ($a=x$). In this case, $\mathcal{H}_c$ has the

additional particle-hole symmetry $\Xi=\tau_x\Theta$ ($\Xi=i\tau_y\Theta$) that satisfies $\Xi^2=\Theta^2$ ($\Xi^2=-\Theta^2$). A similar analysis when $\mathcal{H}_{nc}$ has particle-hole symmetry allows us to conclude that the symmetry class of $\mathcal{H}_c$ is given by a clockwise rotation on the symmetry clock, $s\to s+1$, when θ is a momentum variable. When θ is a position variable, $s\to s-1$ gives a counterclockwise rotation.

Equations (A1) and (A3) map a Hamiltonian into a new Hamiltonian in a different dimension and different symmetry class. It is clear that two Hamiltonians that are topologically equivalent will be mapped to topologically equivalent Hamiltonians since the mapping can be done continuously on a smooth interpolation between the original Hamiltonians. Thus, Eqs. (A1) and (A3) define a mapping between equivalence classes of Hamiltonians. Moreover, since the direct sum of two Hamiltonians is mapped to the direct sum of the new Hamiltonians, the group property of the equivalence classes is preserved. Equations (A1) and (A3) thus define a K-group homomorphism

$$K_{\mathbb{F}}(s;D,d)\to K_{\mathbb{F}}(s+1;D,d+1), \tag{A4}$$

$$K_{\mathbb{F}}(s;D,d)\to K_{\mathbb{F}}(s-1;D+1,d) \tag{A5}$$

for $\mathbb{F}=\mathbb{R},\mathbb{C}$.

2. Invertibility

In order to establish that Eqs. (A4) and (A5) are isomorphisms we need to show that there exists an inverse. This is *not* true of the Hamiltonian mappings. A general Hamiltonian cannot be built from a lower dimensional Hamiltonian using Eqs. (A1) and (A3). However, we will argue that it is possible to continuously deform any Hamiltonian into the form given by Eq. (A1) or (A3). Thus, the mappings between equivalence classes have an inverse. To show this we will use a mathematical method borrowed from Morse theory.[67]

Without loss of generality we again consider *flattened* Hamiltonians having equal number of conduction and valence bands with energies ± 1. Consider $\mathcal{H}(\mathbf{k},\mathbf{r},\theta)$, where $\theta\in[-\pi/2,\pi/2]$ is either a position or momentum variable and $\mathcal{H}$ is independent of $\mathbf{k}$ and $\mathbf{r}$ at $\theta=\pm\pi/2$. We wish to show that $\mathcal{H}(\mathbf{k},\mathbf{r},\theta)$ can be continuously deformed into the form (A1) or (A3). To do so we define an artificial "action"

$$S[\mathcal{H}(\mathbf{k},\mathbf{r},\theta)]=\int d\theta d^d\mathbf{k}d^D\mathbf{r}\ \mathrm{Tr}(\partial_\theta\mathcal{H}\partial_\theta\mathcal{H}). \tag{A6}$$

S can be interpreted as a "height" function in the space of gapped symmetry preserving Hamiltonians. Given any Hamiltonian there is always a downhill direction. These downhill vectors can then be integrated into a deformation trajectory. Since the action is positive definite, it is bounded below. The deformation trajectory must end at a Hamiltonian that locally minimizes the action.

Under the flatness constraint $\mathcal{H}^2=1$, minimal Hamiltonians satisfy the Euler-Lagrange equation

$$\partial_\theta^2\mathcal{H}+\mathcal{H}=0. \tag{A7}$$

The solutions must be a linear combination of $\sin\theta$ and $\cos\theta$. The coefficient of $\sin\theta$ must be constant because the base space is compactified to points at $\theta=\pm\pi/2$. A minimal Hamiltonian thus has the form

$$\mathcal{H}(\mathbf{k},\mathbf{r},\theta)=\cos\theta\mathcal{H}_1(\mathbf{k},\mathbf{r})+\sin\theta\mathcal{H}_0. \tag{A8}$$

The constraint $\mathcal{H}(\mathbf{k},\mathbf{r},\theta)^2=1$ requires

$$\mathcal{H}_0^2=\mathcal{H}_1(\mathbf{k},\mathbf{r})^2=1,\quad \{\mathcal{H}_0,\mathcal{H}_1(\mathbf{k},\mathbf{r})\}=0. \tag{A9}$$

If $\mathcal{H}(\mathbf{k},\mathbf{r},\theta)$ is nonchiral, then Eq. (A8) is already in the form of Eq. (A1) with $\Pi=\mathcal{H}_0$ and $\mathcal{H}_c(\mathbf{k},\mathbf{r})=\mathcal{H}_1(\mathbf{k},\mathbf{r})$. $\mathcal{H}_1$ automatically has chiral symmetry due to Eq. (A9). This shows that Eqs. (A4) and (A5) are invertible when s is odd.

If $\mathcal{H}(\mathbf{k},\mathbf{r},\theta)$ is chiral, then both $\mathcal{H}_0$ and $\mathcal{H}_1(\mathbf{k},\mathbf{r})$ anticommute with the chiral symmetry operator Π. Rename $\mathcal{H}_0=\tau_a$ and $\Pi=i\tau_z\tau_a$, where $a=x$ ($a=y$) when θ is a position (momentum) variable. It follows that $\{\mathcal{H}_1,\tau_x\}=\{\mathcal{H}_1,\tau_y\}=0$ so we can write

$$\mathcal{H}_1(\mathbf{k},\mathbf{r})=h(\mathbf{k},\mathbf{r})\otimes\tau_z. \tag{A10}$$

Equation (A8) thus takes the form of Eq. (A3) with $\mathcal{H}_{nc}=h$. Since τ_z anticommutes with either Θ or Ξ, $h(\mathbf{k},\mathbf{r})$ carries exactly one antiunitary symmetry and is therefore nonchiral. This shows that Eqs. (A4) and (A5) are invertible when s is even.

APPENDIX B: REPRESENTATIVE HAMILTONIANS AND CLASSIFICATION BY WINDING NUMBERS

In this appendix we construct representative Hamiltonians for each of the symmetry classes that are built as linear combinations of Clifford algebra generators that can be represented as anticommuting Dirac matrices. This allows us to relate the integer topological invariants, corresponding to the $\mathbb{Z}$ and $2\mathbb{Z}$ entries in Table I, to the winding degree in maps between spheres. Similar construction for defectless bulk Hamiltonians can be found in Ref. 68 by Ryu, *et al.*. In general, Hamiltonians do not have this specific form. However, since each topological class of Hamiltonians includes representatives of this form, it is always possible to smoothly deform $\mathcal{H}(\mathbf{k},\mathbf{r})$ into this form.

The simplest example of this approach is the familiar case of a two-dimensional Hamiltonian with no symmetries (class A). A topologically nontrivial Hamiltonian can be represented as a 2×2 matrix that can be expressed in terms of Pauli matrices as $\mathcal{H}(\mathbf{k})=\mathbf{h}(\mathbf{k})\cdot\vec{\sigma}$. The Hamiltonian can then be associated with a unit vector $\hat{\mathbf{d}}(\mathbf{k})=\mathbf{h}(\mathbf{k})/|\mathbf{h}(\mathbf{k})|\in S^2$. It is then well known that the Chern number characterizing $\mathcal{H}(\mathbf{k})$ in two dimensions is related to the *degree*, or winding number, of the mapping from $\mathbf{k}$ to S^2. This approach also applies to higher Chern numbers characterizing Hamiltonians in even dimensions $d=2n$. In this case, a Hamiltonian that is a combination of $2n+1$ $2^n\times 2^n$ Dirac matrices, and can be associated with a unit vector $\hat{\mathbf{d}}\in S^{2n}$.

For the complex chiral class AIII, the $U(n)$ winding number characterizing a family of Hamiltonians can similarly be expressed as a winding number on spheres. For example, in $d=1$, a chiral Hamiltonian can be written $\mathcal{H}(k)=h_x(k)\sigma_x+h_y(k)\sigma_y$ (so $\{\mathcal{H},\sigma_z\}=0$), and is characterized by $\hat{\mathbf{d}}(k)\in S^1$.

TABLE V. Examples of Dirac matrices for $(p,q)=(s,0)$.

Classes		Dirac matrices					Symmetry operators		
s	AZ	Γ_0	$\vec{\gamma}$				Θ	Ξ	Π
0	AI	$\mathbb{1}$					K		
1	BDI	σ_z	σ_y				K	$\sigma_x K$	σ_x
2	D	σ_z	σ_y	σ_x				$\sigma_x K$	
3	DIII	$\tau_z\sigma_z$	$\tau_z\sigma_y$	$\tau_z\sigma_x$	τ_x		$i\tau_y\sigma_x K$	$\sigma_x K$	τ_y
4	AII	$\tau_z\sigma_z$	$\tau_z\sigma_y$	$\tau_z\sigma_x$	τ_x	τ_y	$i\tau_y\sigma_x K$		

The integer topological invariant can then be expressed by the winding number of $\hat{\mathbf{d}}(k)$. Similar considerations apply to the integer invariants for chiral Hamiltonians in higher odd dimensions.

For the real symmetry classes we introduce "position-type" Dirac matrices Γ_μ and "momentum-type" Dirac matrices γ_i. These satisfy $\{\Gamma_\mu,\Gamma_\nu\}=2\delta_{\mu\nu}$, $\{\gamma_i,\gamma_j\}=2\delta_{ij}$, and $\{\Gamma_\mu,\gamma_j\}=0$, and are distinguished by their symmetry under antiunitary symmetries. If there is time-reversal symmetry we require

$$[\Gamma_\mu,\Theta]=\{\gamma_i,\Theta\}=0 \tag{B1}$$

while with particle-hole symmetry

$$\{\Gamma_\mu,\Xi\}=[\gamma_i,\Xi]=0. \tag{B2}$$

For a Hamiltonian that is a combination of p momentumlike matrices $\gamma_{1,\ldots,p}$ and $q+1$ positionlike matrices $\Gamma_{0,\ldots,q}$

$$\mathcal{H}(\mathbf{k},\mathbf{r})=\mathbf{R}(\mathbf{k},\mathbf{r})\cdot\vec{\Gamma}+\mathbf{K}(\mathbf{k},\mathbf{r})\cdot\vec{\gamma} \tag{B3}$$

the coefficients must satisfy the involution

$$\mathbf{R}(-\mathbf{k},\mathbf{r})=\mathbf{R}(\mathbf{k},\mathbf{r}), \tag{B4}$$

$$\mathbf{K}(-\mathbf{k},\mathbf{r})=-\mathbf{K}(\mathbf{k},\mathbf{r}). \tag{B5}$$

This can be characterized by a unit vector

$$\hat{\mathbf{d}}(\mathbf{k},\mathbf{r})=\frac{(\mathbf{K},\mathbf{R})}{\sqrt{|\mathbf{K}|^2+|\mathbf{R}|^2}}\in S^{p+q}, \tag{B6}$$

where S^{p+q} is a $(p+q)$ sphere in which p of the dimensions are odd under the involution in Eq. (B5).

The symmetry class s of $\mathcal{H}(\mathbf{k},\mathbf{r})$ is related to the indices (p,q) characterizing the numbers of Dirac matrices by

$$p-q=s \bmod 8. \tag{B7}$$

To see this, start with a Hamiltonian $\mathcal{H}_0=R_0(\mathbf{k},\mathbf{r})\Gamma_0$ that involves a single 1×1 position like "Dirac matrix" $\Gamma_0=\mathbb{1}$ so $(p,q)=(0,0)$. This clearly has time-reversal symmetry, with $\Theta=K$, and corresponds to class AI with $s=0$. Next, generate Hamiltonians $\mathcal{H}_s$ with different symmetries s by using the Hamiltonian mappings introduced in Appendix A. Both the mappings in Eqs. (A1) and (A3) define a new Clifford algebra with one extra generator that is either position or momentum type. The mappings that correspond to clockwise rotations on the symmetry clock $(s\to s+1)$ introduce an additional positionlike generator $(p\to p+1)$ while the mappings that correspond to counterclockwise rotations $(s\to s-1)$ introduce an additional momentumlike generator $(q\to q+1)$. Equation (B7) follows because this procedure can be repeated to generate Hamiltonians with any indices (p,q). Some examples are listed in Table V.

The integer topological invariants in Table I (which occur when $s-\delta$ is even) can be related to the winding degree of the maps $\hat{\mathbf{d}}:S^{D+d}\to S^{p+q}$. This can be nonzero when the spheres have the same total dimensions. In light of Eq. (B7), (p,q) can always be chosen so that $d+D=p+q$. The antiunitary symmetries impose constraints on the possible values of these winding numbers, which depend on the relation between $\delta=d-D$ and $s=p-q$.

The involutions on S^{d+D} and S^{p+q} have opposite orientations when $\delta-s\equiv 2$ or 6 mod 8, and therefore an involution preserving map $S^{d+D}\to S^{p+q}$ can have nonzero winding degree only when $\delta-s\equiv 0$ or 4 mod 8. Symmetry gives a further constraint on the latter case. Consider a sphere map $S^2_{\theta,\phi}\to S^2_{\vartheta,\varphi}$, where the involutions on the spheres send $(\theta,\phi)\mapsto(\theta,\phi+\pi)$ and $(\vartheta,\varphi)\mapsto(\vartheta,\varphi)$. In order for $\varphi(\theta,\phi)=\varphi(\theta,\phi+\pi)$, the winding number must be even. Together, these show

$$\deg\in\begin{cases}\mathbb{Z} & \text{for } \delta-s\equiv 0(\text{mod } 8)\\ 2\mathbb{Z} & \text{for } \delta-s\equiv 4(\text{mod } 8)\\ 0 & \text{otherwise.}\end{cases} \tag{B8}$$

This gives a topological understanding of the $\mathbb{Z}$'s and $2\mathbb{Z}$'s on the periodic table in terms of winding number, which can be identified with the more general analytic invariants, namely, Chern numbers for nonchiral classes

$$n=\frac{1}{\left(\frac{d+D}{2}\right)!}\left(\frac{i}{2\pi}\right)^{(d+D)/2}\int_{T^d\times S^D}\mathrm{Tr}(\mathcal{F}^{(d+D)/2}) \tag{B9}$$

and winding numbers of the chiral flipping operator $q(\mathbf{k},\mathbf{r})$ for chiral ones [see Eqs. (4.1) and (4.2)].

$$n=\frac{\left(\frac{d+D-1}{2}\right)!}{(d+D)!(2\pi i)^{(d+D+1)/2}}\int_{T^d\times S^D}\mathrm{Tr}[(qdq^\dagger)^{d+D}]. \tag{B10}$$

The $\mathbb{Z}_2$'s on the periodic table are not directly characterized by winding degree but rather through dimensional reduction.

Given a Hamiltonian $\mathcal{H}(\mathbf{k},k_1,k_2,\mathbf{r})$ with $s\equiv\delta$ mod 8, its winding degree mod 2 determines the $\mathbb{Z}_2$ classification of its equatorial offspring $\mathcal{H}_{k_2=0}(\mathbf{k},k_1,\mathbf{r})$ and $\mathcal{H}_{k_{1,2}=0}(\mathbf{k},\mathbf{r})$. For example, topological insulators in two and three dimensions are equatorial restrictions of a four-dimensional model $\hat{\mathbf{d}}:S^4\xrightarrow{=}S^4$ with unit winding number. Around the north pole, the Hamiltonian has the form

$$\mathcal{H}(\mathbf{k},k_4)=(m+\varepsilon k^2)\mu_1+\mathbf{k}\cdot\mu_3\vec{\sigma}+k_4\mu_2 \tag{B11}$$

and on the equator $k_4=0$, this gives a three-dimensional Dirac theory of mass m around $\mathbf{k}=\mathbf{0}$ that locally describes 3D topological insulators Bi_2Se_3 and Bi_2Te_3 around Γ.

APPENDIX C: ZERO MODES IN THE HARMONIC OSCILLATOR MODEL

We present exact solvable soliton states of Dirac-type defect Hamiltonians. These include zero modes at a point defect of a Hamiltonian in the chiral class AIII and chiral modes along a line defect of a Hamiltonian in the nonchiral class A. We establish the connection between the two kinds of boundary modes through the Hamiltonian mapping in Eq. (A1).

A nontrivial chiral Hamiltonian isotropic around a point defect at $\mathbf{r}=0$ is a Dirac operator

$$\mathcal{H}=-i\vec{\gamma}\cdot\nabla+\mathbf{r}\cdot\vec{\Gamma}, \tag{C1}$$

where the chiral operator is $\Pi=i^d\Pi_{j=1}^d\gamma_j\Gamma_j$ and its adiabatic limit $e^{-i\mathbf{k}\cdot\mathbf{r}}\mathcal{H}e^{i\mathbf{k}\cdot\mathbf{r}}=\mathbf{k}\cdot\vec{\gamma}+\mathbf{r}\cdot\vec{\Gamma}$ has unit winding degree on $S^{2d-1}=\{(\mathbf{k},\mathbf{r}):k^2+r^2=1\}$.

$$\mathcal{H}^2=-\nabla^2+r^2-i\vec{\gamma}\cdot\vec{\Gamma} \tag{C2}$$

and the spectrum is determined by the quantum numbers $n_j\geq 0$ of the harmonic oscillator and the parities ξ_j of the mutually commuting matrices $i\gamma_j\Gamma_j$, for $j=1,\ldots,d$.

$$\mathcal{E}^2=\sum_{j=1}^{d}2n_j+1-\xi_j. \tag{C3}$$

The unique zero-energy state $|\Psi_0\rangle$, indexed by $n_j=0$ and $\xi_j=1$, has positive chirality $\Pi=+1$, and is exponentially localized at the point defect as $\Psi_0(\mathbf{r})\propto e^{-1/2r^2}$.

Next we consider a nonchiral Hamiltonian isotropic along a line defect.

$$\mathcal{H}(k_\parallel)=k_\parallel\Pi-i\vec{\gamma}\cdot\nabla+\mathbf{r}\cdot\vec{\Gamma}, \tag{C4}$$

where $k_\parallel$ is parallel to the defect line, $\mathbf{r}$ and ∇ are normal position and derivative. Its adiabatic limit $e^{-i\mathbf{k}\cdot\mathbf{r}}\mathcal{H}(k_\parallel)e^{i\mathbf{k}\cdot\mathbf{r}}=k_\parallel\Pi+\mathbf{k}\cdot\vec{\gamma}+\mathbf{r}\cdot\vec{\Gamma}$ is related to that of Eq. (C1) by (1,1) periodicity and has unit winding degree on $S^{2d}=\{(k_\parallel,\mathbf{k},\mathbf{r}):k_\parallel^2+|\mathbf{k}|^2+|\mathbf{r}|^2=1\}$. The zero mode $|\Psi_0\rangle$ of Eq. (C1) gives rise to a positive chiral mode, $\mathcal{H}(k_\parallel)|\Psi_0\rangle=k_\parallel\Pi|\Psi_0\rangle=+k_\parallel|\Psi_0\rangle$ (Fig. 12).

The two examples verified bulk-boundary correspondence through identifying analytic information of the defect-bound solitons and the topology of slowly spatial modulated theories far away from the defect. The single zero mode of Eq. (C1) and spectral flow of Eq. (C4) are equated to unit winding degree of an adiabatic limit. In general, bulk-boundary correspondence is mathematically summarized by index theorems that associate certain analytic and topological indices of Hamiltonians.[41,45,46,56,86,87]

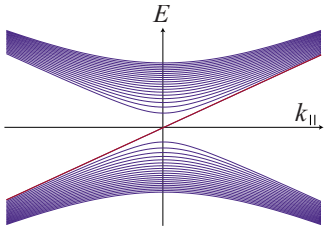

FIG. 12. (Color online) Energy spectrum of Hamiltonian (C4). The zero mode $|\Psi_0\rangle$ of positive chirality at $k_\parallel=0$ corresponds the chiral mode that generates the midgap $k_\parallel$-linear energy spectrum.

APPENDIX D: INVARIANT FOR POINT DEFECTS IN CLASS D AND BDI

We follow the derivation given in Ref. 53, which was based on Qi, Hughes, and Zhang's formulation of the topological invariant characterizing a three-dimensional topological insulator.[10] For a point defect in d dimensions, the Hamiltonian $\mathcal{H}(\mathbf{k},\mathbf{r})$ depends on d momentum variables and $d-1$ position variables. We introduce a one parameter deformation $\tilde{\mathcal{H}}(\lambda,\mathbf{k},\mathbf{r})$ that connects $\tilde{\mathcal{H}}(\mathbf{k},\mathbf{r})$ at $\lambda=0$ to a constant Hamiltonian at $\lambda=1$ while breaking particle-hole symmetry. The particle-hole symmetry can be restored by including a mirror image $\tilde{\mathcal{H}}(\lambda,\mathbf{k},\mathbf{r})=-\Xi\mathcal{H}(-\lambda,\mathbf{k},\mathbf{r})\Xi^{-1}$ for $-1<\lambda<0$. For $\lambda=\pm$, $(\mathbf{k},\mathbf{r})$ can be replaced by a single point, so the $2d$ parameter space $(\lambda,\mathbf{k},\mathbf{r})$ is the suspension $\Sigma(T^d\times S^{d-1})$ of the original space. The Hamiltonian defined on this space is characterized by its dth Chern character

$$\nu=\frac{1}{d!}\left(\frac{i}{2\pi}\right)^d\int_{\Sigma(T^d\times S^{d-1})}\mathrm{Tr}[\mathcal{F}^d]. \tag{D1}$$

Due to particle-hole symmetry, the contributions from the two hemispheres $\lambda>0$, $\lambda<0$ are equal. Using the fact that the integrand is the derivative of the Chern Simons form, $\mathrm{Tr}[\mathcal{F}^d]=d\mathcal{Q}_{2d-1}$, we can therefore write

$$\nu=\frac{2}{d!}\left(\frac{i}{2\pi}\right)^d\int_{T^d\times S^{d-1}}\mathcal{Q}_{2d-1}. \tag{D2}$$

As was the case in Refs. 10 and 53, ν can be different for different deformations $\mathcal{H}(\lambda,\mathbf{k},\mathbf{r})$. However, particle-hole symmetry requires the difference is an even integer. Thus, the parity of Eq. (D2) defines the $\mathbb{Z}_2$ invariant.

The Chern Simons form $\mathcal{Q}_{2d-1}$ can be expressed in terms of the connection $\mathcal{A}$ via the general formula

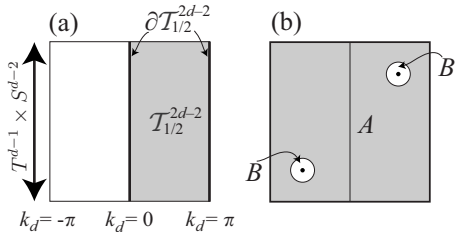

FIG. 13. (a) Schematic of the base space $\mathcal{T}^{2d-2}=T^d\times S^{d-2}$, split into two halves. (b) Division of $\mathcal{T}^{2d-2}$ into patches A and B, each closed under TR and has an individual valence frame $|u_m^{A/B}\rangle$ that satisfies the gauge condition in Eq. (E2).

$$\mathcal{Q}_{2d-1}=d\int_0^1 dt\ \mathrm{Tr}[\mathcal{A}(td\mathcal{A}+t^2\mathcal{A}^2)^{d-1}]. \tag{D3}$$

In the addition of time-reversal symmetry $\Theta^2=1$ or equivalently a chiral symmetry $\Pi=\Theta\Pi=\tau_z$, a valence frame of the BDI Hamiltonian (4.1) can be chosen to be

$$u(\mathbf{k},\mathbf{r})=\frac{1}{\sqrt{2}}\begin{pmatrix} q(\mathbf{k},\mathbf{r}) \\ -\mathbb{1}\end{pmatrix}, \tag{D4}$$

where q is unitary and $\mathbb{1}$ is the identity matrix. This corresponds the Berry connection $\mathcal{A}=u^\dagger du=\frac{1}{2}q^\dagger dq$ and Chern-Simons form

$$\mathcal{Q}_{2d-1}=\frac{d}{2}\int_0^1 dt\left[\frac{t}{2}\left(\frac{t}{2}-1\right)\right]^{d-1}\mathrm{Tr}[(q^\dagger dq)^{2d-1}]$$

$$=\frac{(-1)^d}{2}\frac{d!(d-1)!}{(2d-1)!}\mathrm{Tr}[(q^\dagger dq)^{2d-1}]. \tag{D5}$$

This equates the winding number of q in Eq. (4.2) to the Chern Simons invariant in Eq. (4.9).

APPENDIX E: INVARIANT FOR LINE DEFECTS IN CLASS AII AND POINT DEFECTS IN DIII

We formulate a topological invariant that characterizes line defects in class AII in all dimensions that is analogous to the integral formula invariant characterizing the quantum spin-Hall insulator introduced in Ref. 73. This can be applied to weak topological insulators in three dimensions with dislocation around a line defect. The invariant can be indirectly applied to strong topological insulators through decomposition into strong and weak components. As a consequence of the Hamiltonian mapping in Eq. (A1) that identifies ($s=4$, $\delta=2$) and ($s=3$, $\delta=1$), this gives a new topological invariant that classified point defects in class DIII in all dimensions.

1. Line defects in class AII

The base space manifold is $\mathcal{T}^{2d-2}=T^d\times S^{d-2}$, where T^d is the Brillouin zone and $S^{d-2}\times\mathbb{R}$ is a cylindrical neighborhood that wraps around the line defect in real space. Divide the base space into two pieces, $\mathcal{T}_{1/2}^{2d-2}$ and its time reversal counterpart [see Fig. 13(a)]. We will show the $\mathbb{Z}_2$ invariant

$$\nu=\frac{i^{d-1}}{(d-1)!(2\pi)^{d-1}}\left[\int_{\mathcal{T}_{1/2}^{2d-2}}\mathrm{Tr}(\mathcal{F}^{d-1})-\oint_{\partial\mathcal{T}_{1/2}^{2d-2}}\mathcal{Q}_{2d-3}\right] \tag{E1}$$

topologically classifies line defects in AII, where the Chern-Simons form, defined by Eq. (D3), is generated by the Berry connection $\mathcal{A}_{mn}=\langle u_m(\mathbf{k},\mathbf{r})|du_n(\mathbf{k},\mathbf{r})\rangle$, and the valence frame $u_m(\mathbf{k},\mathbf{r})$ satisfies the gauge condition

$$w_{mn}(\mathbf{k},\mathbf{r})=\langle u_m(\mathbf{k},\mathbf{r})|\Theta u_n(-\mathbf{k},\mathbf{r})\rangle=\text{constant} \tag{E2}$$

on the boundary $(\mathbf{k},\mathbf{r})\in\partial\mathcal{T}_{1/2}^{2d-2}$.

The nontriviality of the $\mathbb{Z}_2$ invariant is a topological obstruction to choosing a global continuous valence frame $|u_m(\mathbf{k},\mathbf{r})\rangle$ that satisfies the gauge condition in Eq. (E2) on the whole base space $\mathcal{T}^{2d-2}$. If there is no topological obstruction from the bulk,[88] the gauge condition forces the valence frame to be singular at two points, depicted in Fig. 13(b), related to each other by time reversal. One removes the singularity by picking another valence frame locally defined on two small balls enclosing the two singular points, denoted by B in Fig. 13(b). We therefore have two valence frames $|u_m^{A/B}(\mathbf{k},\mathbf{r})\rangle$ defined on two patches of the base space, $A=\mathcal{T}^{2d-2}\backslash B$ and B, each obeying the gauge condition in Eq. (E2).

The wave functions on the two patches translate into each other through transition function

$$t_{mn}^{AB}(\mathbf{k},\mathbf{r})=\langle u_m^A(\mathbf{k},\mathbf{r})|u_n^B(\mathbf{k},\mathbf{r})\rangle\in U(k) \tag{E3}$$

on the boundary $\partial B\approx S^{2d-3}\cup S^{2d-3}$. The function behavior on the two disjoint $(2d-3)$ spheres is related by time reversal. The topology is characterized by the winding of $t^{AB}:S^{2d-3}\to U(k)$ on one of the spheres

$$\nu=\frac{(d-2)!}{(2d-3)!(2\pi i)^{d-1}}\oint_{S^{2d-3}}\mathrm{Tr}[(t^{AB}d(t^{AB})^\dagger)^{2d-3}], \tag{E4}$$

$$=\frac{(-1)^d}{(d-1)!(2\pi i)^{d-1}}\oint_{S^{2d-3}}(\mathcal{Q}_{2d-3}^A-\mathcal{Q}_{2d-3}^B). \tag{E5}$$

The two integrals can be evaluated separately. Since $d\mathcal{Q}_{2d-3}=\mathrm{Tr}(\mathcal{F}^{d-1})$, Stokes' theorem tells us

$$\int_{A\cap\mathcal{T}_{1/2}^{2d-2}}\mathrm{Tr}(\mathcal{F}^{d-1})=\left(\oint_{\partial\mathcal{T}_{1/2}^{2d-2}}-\oint_{S^{2d-3}}\right)\mathcal{Q}_{2d-3}^A,$$

$$\int_{B\cap\mathcal{T}_{1/2}^{2d-2}}\mathrm{Tr}(\mathcal{F}^{d-1})=\oint_{S^{2d-3}}\mathcal{Q}_{2d-3}^B.$$

Combining these into Eq. (E5) identifies the $\mathbb{Z}_2$ invariant in Eq. (E1) with the winding number of the transition function.

The curvature term in Eq. (E1) is gauge invariant. Any gauge transformation on the boundary $\partial\mathcal{T}_{1/2}^{2d-2}$ respecting the gauge condition in Eq. (E2) has even winding number and would alter the Chern-Simons integral by an even integer. The gauge condition is therefore essential to make the formula nonvacuous.

Spin Chern number

A quantum spin-Hall insulator is characterized by its spin Chern number $n_\sigma=(n_\uparrow-n_\downarrow)/2$. We generalize this to time-reversal invariant line defects of all dimensions by equating it with Eq. (E1). This applies in particular to a model we considered for a linear Josephson junction in Sec. III D.

A spin operator S is a unitary operator, square to unity, commutes with the Hamiltonian, and anticommutes with the time reversal operator. The valence spin frame

$$|u_m^\downarrow(\mathbf{k},\mathbf{r})\rangle = \Theta|u_m^\uparrow(-\mathbf{k},\mathbf{r})\rangle \tag{E6}$$

automatically satisfies the time reversal gauge constraint in Eq. (E2). It is straightforward to check that the curvature and Chern-Simons form can be split as direct sums according to spins.

$$\mathcal{F}(\mathbf{k},\mathbf{r}) = \mathcal{F}^\uparrow(\mathbf{k},\mathbf{r}) \oplus \mathcal{F}^\uparrow(-\mathbf{k},\mathbf{r})^*, \tag{E7}$$

$$\mathcal{Q}_{2d-3}(\mathbf{k},\mathbf{r}) = \mathcal{Q}_{2d-3}^\uparrow(\mathbf{k},\mathbf{r}) \oplus \mathcal{Q}_{2d-3}^\uparrow(-\mathbf{k},\mathbf{r})^*. \tag{E8}$$

Again assuming that there is no lower dimensional "weak" topology, the $\uparrow$ frame can be defined everywhere on $\mathcal{T}^{2d-2}$ with a singularity at one point, say, in $\mathcal{T}_{1/2}^{2d-2}$, and the $\downarrow$ frame is singular only at the time reversal of that point.

The curvature term of Eq. (E1) splits into two terms

$$\int_{\mathcal{T}_{1/2}^{2d-2}} \mathrm{Tr}(\mathcal{F}^{d-1}) = \left[\int_{\mathcal{T}_{1/2}^{2d-2}} - \int_{\mathcal{T}^{2d-2}\setminus\mathcal{T}_{1/2}^{2d-2}}\right] \mathrm{Tr}(\mathcal{F}_\uparrow^{d-1}) \tag{E9}$$

and the two spin components of the Chern-Simons term $\oint_{\partial\mathcal{T}_{1/2}^{2d-2}}\mathcal{Q}_{2d-3}$ add up into

$$2\oint_{\partial\mathcal{T}_{1/2}^{2d-2}} \mathcal{Q}_{2d-3}^\uparrow = -2\int_{\mathcal{T}^{2d-2}\setminus\mathcal{T}_{1/2}^{2d-2}} \mathrm{Tr}(\mathcal{F}_\uparrow^{d-1}) \tag{E10}$$

by Stokes theorem.

Combining these two, we equate Eq. (E1) to the spin Chern number

$$n_\uparrow = \frac{i^{d-1}}{(d-1)!2\pi^{d-1}}\int_{\mathcal{T}^{2d-2}} \mathrm{Tr}(\mathcal{F}_\uparrow^{d-1}). \tag{E11}$$

Time reversal requires $n_{tot}=n_\uparrow+n_\downarrow=0$ and therefore $n_\sigma=(n_\uparrow-n_\downarrow)/2=n_\uparrow$.

2. Point defects in class DIII

The base space manifold is $\mathcal{T}^{2d-1}=T^d\times S^{d-1}$. The Hamiltonian mapping in Eq. (A1) relates a point-defect Hamiltonian $\mathcal{H}(\mathbf{k},\mathbf{r})$ in class DIII to a line-defect Hamiltonian $\mathcal{H}(\mathbf{k},\mathbf{r},\theta)=\cos\theta\mathcal{H}(\mathbf{k},\mathbf{r})+\sin\theta\Pi$ in class AII, where $\Pi=i\Theta\Xi$ is the chiral operator, $(\mathbf{k},\mathbf{r},\theta)\in\Sigma\mathcal{T}^{2d-1}$ [see Fig. 14(a)] and θ is odd under time reversal. The line defect Hamiltonian $\mathcal{H}(\mathbf{k},\mathbf{r},\theta)$ is topologically characterized by the generalization of Eq. (E1), which was proven to be identical to the winding number in Eq. (E4) of the transition function t^{AB} [see Fig. 14(b) for the definition of patches A and B]. We will utilize this to construct a topological invariant that characterizes point defects in class DIII.

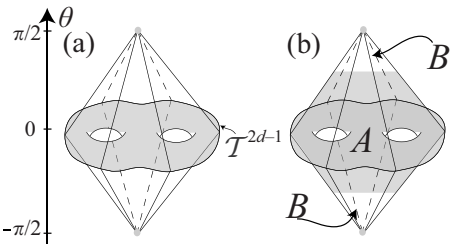

FIG. 14. (a) Schematic of the suspension $\Sigma\mathcal{T}^{2d-1}$. (b) Decomposition into patches A and B.

Set $\Theta=\tau_y K$ and $\Xi=\tau_x K$ under an appropriate choice of basis. A *canonical* valence frame of $\mathcal{H}(\mathbf{k},\mathbf{r},\theta)$ can be chosen to be

$$u_+^B(\mathbf{k},\mathbf{r},\theta) = \begin{pmatrix} \sin\left(\frac{\pi}{4}-\frac{\theta}{2}\right)q(\mathbf{k},\mathbf{r}) \\ -\cos\left(\frac{\pi}{4}-\frac{\theta}{2}\right)\mathbb{1} \end{pmatrix}, \tag{E12}$$

where $q(\mathbf{k},\mathbf{r})\in U(k)$ is from the canonical form of the chiral Hamiltonian $\mathcal{H}(\mathbf{k},\mathbf{r})$ in Eq. (4.1), $\mathbb{1}$ is the $k\times k$ identity matrix, and the valence frame is nonsingular everywhere except at $\theta=-\pi/2$. There is a gauge transformation $u_+^B\to u^A=u_+^B t^{BA}$ everywhere except $\theta=\pm\pi/2$ such that the new frame u^A satisfies the gauge condition in Eq. (E2).[89] A valence frame on patch B can be constructed by requiring $u_-^B(\theta)=\Theta u_+^B(-\theta)$ around $\theta=-\pi/2$.

The $\mathbb{Z}_2$ topology is characterized by the evenness or oddness of the winding number of t^{AB} as in Eq. (E4). This can be evaluated by the integral along the equator $\theta=0$

$$\tilde{\nu} = \frac{(d-1)!}{(2d-1)!(2\pi i)^d}\int_{T^d\times S^{d-1}} \mathrm{Tr}\{[t^{AB}d(t^{AB})^\dagger]^{2d-1}\}, \tag{E13}$$

where $u^A=u_+^B t^{BA}$ is a solution to the gauge condition in Eq. (E2) or equivalently t^{BA} satisfies

$$q(\mathbf{k},\mathbf{r}) = t^{BA}(-\mathbf{k},\mathbf{r})\sigma_y t^{BA}(\mathbf{k},\mathbf{r})^T, \tag{E14}$$

where the constant in Eq. (E2) is chosen to be $i\sigma_y$.

The winding number in Eq. (E13) can also be expressed as a Chern-Simons integral.

$$\tilde{\nu} = \frac{i^d}{d!(2\pi)^d}\int_{T^d\times S^{d-1}} (\mathcal{Q}_{2d-1}^B - \mathcal{Q}_{2d-1}^A), \tag{E15}$$

where $\mathcal{Q}^{A/B}$ are the Chern-Simons form generated by valence frames $u^{A/B}$. Restricted to $\theta=0$, Eq. (E12) gives $u^B(\mathbf{k},\mathbf{r})=\frac{1}{\sqrt{2}}(q(\mathbf{k},\mathbf{r}),-\mathbb{1})$. Following Eq. (D5), the first term of Eq. (E15) equals half of the winding number of q, which is guaranteed to be zero by time-reversal and particle-hole symmetries. And therefore point defects in DIII are classified by the Chern-Simons invariant

$$\tilde{\nu} = \frac{1}{d!}\left(\frac{i}{2\pi}\right)^d \int_{T^d \times S^{d-1}} \mathcal{Q}_{2d-1} \bmod 2, \tag{E16}$$

where the Chern-Simons form is generated by a valence frame that satisfies the time-reversal gauge constraint in Eq. (E2).

Note that the integrality of the Chern-Simons integral in Eq. (E16) is a result of particle-hole symmetry. Forgetting time reversal symmetry, point defects in class D are classified by the Chern-Simons invariant $\nu = 2\tilde{\nu}$ in Eq. (D2) with a factor of 2. Time-reversal symmetry requires the zero modes to form Kramers doublets and therefore $\nu = 2\tilde{\nu}$ must be even. A gauge transformation in general can alter $\tilde{\nu}$ by any integer. Thus, similar to the formula in class AII, the time-reversal gauge constraint in Eq. (E2) is essential so that Eq. (E16) is nonvacuous.

Fixed points formula in 1D

We here identify Eq. (E16), or equivalently Eq. (E13), to a fixed point invariant in 1 dimension. In Ref. 82, Qi, Hughes, and Zhang showed that 1D time reversal invariant superconductors are $\mathbb{Z}_2$ classified by the topological invariant

$$(-1)^{\tilde{\nu}} = \frac{\mathrm{Pf}(q_{k=\pi})}{\mathrm{Pf}(q_{k=0})} \exp\left[\frac{1}{2}\int_0^{\pi} \mathrm{Tr}(q_k dq_k^\dagger)\right] \tag{E17}$$

under the basis $\Theta = \tau_y K$ and $\Xi = \tau_x K$, where q_k is the chiral flipping operator in Eq. (4.1). Time-reversal and particle-hole symmetries requires $q_k = -q_{-k}^T$. Hence the Pfaffians are well defined as q_k is antisymmetric at the fixed points $k = 0, \pi$.

Using the gauge condition in Eq. (E14), we can expressed the Pfaffians as $\mathrm{Pf}(\Theta q_{k=0,\pi}) = \det(t_{k=0,\pi})\mathrm{Pf}(\sigma_y)$, where t_k^{BA} is abbreviated to t_k.

$$\frac{\mathrm{Pf}(q_{k=\pi})}{\mathrm{Pf}(q_{k=0})} = \exp\left[-\int_0^{\pi} \mathrm{Tr}(t_k dt_k^\dagger)\right]. \tag{E18}$$

Substitute Eq. (E14) into the Cartan form $\mathrm{Tr}(q_k dq_k^\dagger)$ gives

$$\mathrm{Tr}(q_k dq_k^\dagger) = \mathrm{Tr}(t_{-k} dt_{-k}^\dagger) + \mathrm{Tr}(t_k dt_k^\dagger). \tag{E19}$$

Combining these into Eq. (E17)

$$(-1)^{\tilde{\nu}} = \exp\left[\frac{1}{2}\int_0^{\pi} \mathrm{Tr}(t_{-k} dt_{-k}^\dagger - t_k dt_k^\dagger)\right], \tag{E20}$$

$$= \exp\left[-\frac{1}{2}\int_{-\pi}^{\pi} \mathrm{Tr}(t_k dt_k^\dagger)\right], \tag{E21}$$

which agrees Eq. (E13).

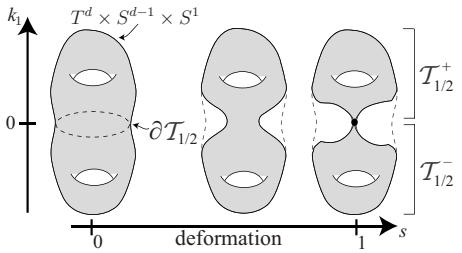

FIG. 15. Deformation of Hamiltonian and its base manifold so that the boundary $\partial\mathcal{T}_{1/2}$ is shrink to a point.

APPENDIX F: INVARIANT FOR FERMION PARITY PUMPS

In the appendix, we will show that a $\mathbb{Z}_2$ invariant in Eq. (5.2) under a particle-hole gauge constraint topologically classified fermion parity pumps in dimension $\delta = 0$ and class D or BDI. (See Sec. V B for the full statement.) We will show Eq. (5.2) using a construction similar to a reasoning in Moore and Balents.[7] We consider a deformation of the Hamiltonian along with the base manifold so that the boundary $\partial\mathcal{T}_{1/2}$ is deformed into a single point (see Fig. 15). Let $s \in [0,1]$ be the deformation variable, and denote $\mathcal{T}_{1/2}^+(s)$ and $\partial\mathcal{T}_{1/2}(s)$ be the corresponding deformation slices. Chern invariant

$$n = \frac{1}{d!}\left(\frac{i}{2\pi}\right)^d \int_{\mathcal{T}_{1/2}^+(s=1)} \mathrm{Tr}(\mathcal{F}^d) \tag{F1}$$

integrally classifies Hamiltonians on the half-manifold $\mathcal{T}_{1/2}^+(s=1)$. Particle-hole symmetry requires opposite Chern invariant on the other half. A different choice of deformation could only change the Chern invariant by an even integer.[90] Hence the Chern invariant modulo 2 defines a $\mathbb{Z}_2$ invariant.

The Chern integral can be further deformed and decomposed into

$$\int_{\mathcal{T}_{1/2}^+(s=0)} \mathrm{Tr}(\mathcal{F}^d) + \int_0^1 ds \int_{\partial\mathcal{T}_{1/2}^+(s)} \mathrm{Tr}(\mathcal{F}^d)$$
$$= \int_{\mathcal{T}_{1/2}^+(s=0)} \mathrm{Tr}(\mathcal{F}^d) - \oint_{\partial\mathcal{T}_{1/2}^+(s=0)} \mathcal{Q}_{2d-1}, \tag{F2}$$

where Stokes' theorem is used and the negative sign is from a change in orientation of the boundary. This proves Eq. (5.2). The particle-hole gauge constraint is built-in since the $G_{\mathbf{k},\mathbf{r},t}(s)$ deforms into a constant at $s=1$ while respecting particle-hole symmetry in Eq. (5.4) at all s.

[1] D. J. Thouless, M. Kohmoto, M. P. Nightingale, and M. den Nijs, Phys. Rev. Lett. **49**, 405 (1982).
[2] X. L. Qi and S. C. Zhang, Phys. Today **63**(1), 33 (2010).
[3] J. E. Moore, Nature (London) **464**, 194 (2010).
[4] M. Z. Hasan and C. L. Kane, arXiv:1002.3895v1 (unpublished).
[5] C. L. Kane and E. J. Mele, Phys. Rev. Lett. **95**, 226801 (2005).
[6] C. L. Kane and E. J. Mele, Phys. Rev. Lett. **95**, 146802 (2005).
[7] J. E. Moore and L. Balents, Phys. Rev. B **75**, 121306(R) (2007).

[8] R. Roy, Phys. Rev. B **79**, 195322 (2009).
[9] L. Fu, C. L. Kane, and E. J. Mele, Phys. Rev. Lett. **98**, 106803 (2007).
[10] X. L. Qi, T. L. Hughes, and S. C. Zhang, Phys. Rev. B **78**, 195424 (2008).
[11] A. Bernevig, T. Hughes, and S. C. Zhang, Science **314**, 1757 (2006).
[12] L. Fu and C. L. Kane, Phys. Rev. B **76**, 045302 (2007).
[13] H. Zhang, C. X. Liu, X. L. Qi, X. Dai, Z. Fang, and S. C. Zhang, Nat. Phys. **5**, 438 (2009).
[14] M. König, S. Wiedmann, C. Brüne, A. Roth, H. Buhmann, L. W. Molenkamp, X.-L. Qi, and S.-C. Zhang, Science **318**, 766 (2007).
[15] M. König, H. Buhmann, L. W. Molenkamp, T. Hughes, C.-X. Liu, X.-L. Qi, and S.-C. Zhang, J. Phys. Soc. Jpn. **77**, 031007 (2008).
[16] A. Roth, C. Brüne, H. Buhmann, L. W. Molenkamp, J. Maciejko, X. L. Qi, and S. C. Zhang, Science **325**, 294 (2009).
[17] D. Hsieh, D. Qian, L. Wray, Y. Xia, Y. S. Hor, R. J. Cava, and M. Z. Hasan, Nature (London) **452**, 970 (2008).
[18] D. Hsieh, Y. Xia, L. Wray, D. Qian, A. Pal, J. H. Dil, J. Osterwalder, F. Meier, G. Bihlmayer, C. L. Kane, Y. S. Hor, R. J. Cava, and M. Z. Hasan, Science **323**, 919 (2009).
[19] P. Roushan, J. Seo, C. V. Parker, Y. S. Hor, D. Hsieh, D. Qian, A. Richardella, M. Z. Hasan, R. J. Cava, and A. Yazdani, Nature (London) **460**, 1106 (2009).
[20] Y. Xia, D. Qian, D. Hsieh, L. Wray, A. Pal, H. Lin, A. Bansil, D. Grauer, Y. S. Hor, R. J. Cava, and M. Z. Hasan, Nat. Phys. **5**, 398 (2009).
[21] Y. S. Hor, A. Richardella, P. Roushan, Y. Xia, J. G. Checkelsky, A. Yazdani, M. Z. Hasan, N. P. Ong, and R. J. Cava, Phys. Rev. B **79**, 195208 (2009).
[22] Y. L. Chen, J. G. Analytis, J. H. Chu, Z. K. Liu, S. K. Mo, X. L. Qi, H. J. Zhang, D. H. Lu, X. Dai, Z. Fang, S. C. Zhang, I. R. Fisher, Z. Hussain, and Z. X. Shen, Science **325**, 178 (2009).
[23] D. Hsieh, Y. Xia, D. Qian, L. Wray, J. H. Dil, F. Meier, J. Osterwalder, L. Patthey, J. G. Checkelsky, N. P. Ong, A. V. Fedorov, H. Lin, A. Bansil, D. Grauer, Y. S. Hor, R. J. Cava, and M. Z. Hasan, Nature (London) **460**, 1101 (2009).
[24] S. R. Park, W. S. Jung, C. Kim, D. J. Song, C. Kim, S. Kimura, K. D. Lee, and N. Hur, Phys. Rev. B **81**, 041405(R) (2010).
[25] Z. Alpichshev, J. G. Analytis, J. H. Chu, I. R. Fisher, Y. L. Chen, Z. X. Shen, A. Fang, and A. Kapitulnik, Phys. Rev. Lett. **104**, 016401 (2010).
[26] D. Hsieh, Y. Xia, D. Qian, L. Wray, F. Meier, J. H. Dil, J. Osterwalder, L. Patthey, A. V. Fedorov, H. Lin, A. Bansil, D. Grauer, Y. S. Hor, R. J. Cava, and M. Z. Hasan, Phys. Rev. Lett. **103**, 146401 (2009).
[27] A. Shitade, H. Katsura, J. Kunes, X. L. Qi, S. C. Zhang, and N. Nagaosa, Phys. Rev. Lett. **102**, 256403 (2009).
[28] R. Li, J. Wang, X. L. Qi, and S. C. Zhang, Nat. Phys. **6**, 376 (2010).
[29] S. Chadov, X. L. Qi, J. Kübler, G. H. Fecher, C. Felser, and S. C. Zhang, Nature Mater. **9**, 541 (2010).
[30] H. Lin, L. A. Wray, Y. Xia, S. Xu, S. Jia, R. J. Cava, A. Bansil, and M. Z. Hasan, Nature Mater. **9**, 546 (2010).
[31] H. Lin, L. A. Wray, Y. Xia, S. Y. Xu, S. Jia, R. J. Cava, A. Bansil, and M. Z. Hasan, arXiv:1003.2615 (unpublished).
[32] H. Lin, L. A. Wray, Y. Xia, S. Y. Xu, S. Jia, R. J. Cava, A. Bansil, and M. Z. Hasan, arXiv:1004.0999 (unpublished).
[33] B. Yan, C. X. Liu, H. J. Zhang, C. Y. Yam, X. L. Qi, T. Frauenheim, and S. C. Zhang, arXiv:1003.0074 (unpublished).
[34] R. Roy, arXiv:0803.2868 (unpublished).
[35] A. P. Schnyder, S. Ryu, A. Furusaki, and A. W. W. Ludwig, Phys. Rev. B **78**, 195125 (2008); AIP Conf. Proc. **1134**, 10 (2009).
[36] A. Kitaev, AIP Conf. Proc. **1134**, 22 (2009).
[37] X. L. Qi, T. L. Hughes, S. Raghu, and S. C. Zhang, Phys. Rev. Lett. **102**, 187001 (2009).
[38] A. Kitaev, arXiv:cond-mat/0010440 (unpublished).
[39] N. Read and D. Green, Phys. Rev. B **61**, 10267 (2000).
[40] A. P. Mackenzie and Y. Maeno, Rev. Mod. Phys. **75**, 657 (2003).
[41] G. E. Volovik, *The Universe in a Helium Droplet* (Clarendon, Oxford, 2003).
[42] G. E. Volovik, JETP Lett. **90**, 587 (2009).
[43] P. Hořava, Phys. Rev. Lett. **95**, 016405 (2005).
[44] A. Altland and M. R. Zirnbauer, Phys. Rev. B **55**, 1142 (1997).
[45] R. Jackiw and C. Rebbi, Phys. Rev. D **13**, 3398 (1976).
[46] R. Jackiw and P. Rossi, Nucl. Phys. B **190**, 681 (1981).
[47] W. P. Su, J. R. Schrieffer, and A. J. Heeger, Phys. Rev. Lett. **42**, 1698 (1979).
[48] L. Fu and C. L. Kane, Phys. Rev. Lett. **100**, 096407 (2008).
[49] J. D. Sau, R. M. Lutchyn, S. Tewari, and S. Das Sarma, Phys. Rev. Lett. **104**, 040502 (2010).
[50] J. Alicea, Phys. Rev. B **81**, 125318 (2010).
[51] R. M. Lutchyn, J. D. Sau, and S. Das Sarma, Phys. Rev. Lett. **105**, 077001 (2010).
[52] Y. Oreg, G. Refael, and F. von Oppen, arXiv:1003.1145 (unpublished).
[53] J. C. Y. Teo and C. L. Kane, Phys. Rev. Lett. **104**, 046401 (2010).
[54] M. Nakahara, *Geometry, Topology and Physics* (Adam Hilger, Bristol, 1990).
[55] J. Goldstone and F. Wilczek, Phys. Rev. Lett. **47**, 986 (1981).
[56] E. J. Weinberg, Phys. Rev. D **24**, 2669 (1981).
[57] E. Witten, Phys. Lett. **117B**, 324 (1982).
[58] E. Witten, J. Diff. Geom. **17**, 611 (1982).
[59] S. C. Davis, A. C. Davis, and W. B. Perkins, Phys. Lett. **408B**, 81 (1997).
[60] D. J. Thouless, Phys. Rev. B **27**, 6083 (1983).
[61] Q. Niu and D. J. Thouless, J. Phys. A **17**, 2453 (1984).
[62] M. Freedman, M. B. Hastings, C. Nayak, X. L. Qi, K. Walker, and Z. Wang, arXiv:1005.0583 (unpublished).
[63] M. Karoubi, *K-Theory: An Introduction* (Springer-Verlag, Berlin, 1978).
[64] H. B. Lawson and M. L. Michelsohn, *Spin Geometry* (Princeton University Press, Princeton, 1989).
[65] M. Atiyah, *K Theory* (Westview Press, Boulder, CO, 1994).
[66] R. Bott, Ann. Math. **70**, 313 (1959).
[67] J. Milnor, *Morse Theory* (Princeton University Press, Princeton, 1963).
[68] S. Ryu, A. Schnyder, A. Furusaki, and A. W. W. Ludwig, New J. Phys. **12**, 065010 (2010).
[69] E. I. Blount, Solid State Phys. **13**, 305 (1962).
[70] R. Li, J. Wang, X. L. Qi, and S. C. Zhang, Nat. Phys. **6**, 284 (2010).
[71] R. S. K. Mong, A. M. Essin, and J. E. Moore, Phys. Rev. B **81**, 245209 (2010).
[72] G. E. Volovik, Pis'ma Zh. Eksp. Teor. Fiz. **91**, 61 (2010); arXiv:1001.1514 (unpublished).

[73] L. Fu and C. L. Kane, Phys. Rev. B **74**, 195312 (2006).
[74] T. Fukui and T. Fujiwara, J. Phys. A **42**, 362003 (2009).
[75] Y. Ran, Y. Zhang, and A. Vishwanath, Nat. Phys. **5**, 298 (2009).
[76] P. G. Grinevich and G. E. Volovik, J. Low Temp. Phys. **72**, 371 (1988).
[77] M. A. Silaev and G. E. Volovik, arXiv:1005.4672 (unpublished).
[78] R. B. Laughlin, Phys. Rev. Lett. **80**, 5188 (1998).
[79] L. S. Pontrjagin, Rec. Math. [Mat. Sbornik] N.S. **9**, 331 (1941) [http://mathnet.ru/mst6073].
[80] J. Jäykkä and J. Hietarinta, Phys. Rev. D **79**, 125027 (2009).
[81] L. Kapitanski, London Mathematical Society Durham Symposium (unpublished).
[82] X. L. Qi, T. L. Hughes, and S. C. Zhang, Phys. Rev. B **81**, 134508 (2010).
[83] L. Fu, and C. L. Kane, Phys. Rev. B **79**, 161408(R)(2009).
[84] Y. Ran, P. Hosur, and A. Vishwanath, arXiv:1003.1964 (unpublished).
[85] R. B. Laughlin, Phys. Rev. B **23**, 5632(R) (1981).
[86] T. Fukui and T. Fujiwara, J. Phys. Soc. Jpn. **79**, 033701 (2010).
[87] T. Fukui, Phys. Rev. B **81**, 214516 (2010).
[88] Bulk topology is a lower dimenional topological obstruction coming purely from the momentum part T^d of the base space $T^d \times S^{d-2}$. One could mathematically remove the bulk topological obstruction by adding a defectless Hamiltonian $\tilde{\mathcal{H}}(\mathbf{k},\mathbf{r}) = \mathcal{H}(\mathbf{k},\mathbf{r}) \oplus \mathcal{H}_0(\mathbf{k})$.
[89] Again, assume the bulk has trivial topology. Or otherwise remove the topological obstruction mathematically by adding a defectless Hamiltonian.
[90] Deformation of Hamiltonians on $\partial\mathcal{T}_{1/2}(s)$, for $s \in [0,1]$ has dimension $\delta=(d-1)-(d-1+1+1)=-2$, and is classified by $2\mathbb{Z}$.